

2-Arylimino-9-phenyl-1,10-phenanthroline-iron, -cobalt and -nickel Complexes: Synthesis, Characterization and Ethylene Oligomerization Behavior

Suyun Jie,^[a] Shu Zhang,^[a] and Wen-Hua Sun*^[a]

Keywords: Nitrogen ligands / Late transition metals / Iron / Ethylene / Oligomerization

A series of 2-imino-9-phenyl-1,10-phenanthrolines **1–6** has been prepared and investigated as new tridentate N₃ ligands in coordination with metal chlorides. Their iron(II) (**1a–6a**), cobalt(II) (**1b–6b**), and nickel(II) (**1c–6c**) complexes have been synthesized and characterized by elemental and spectroscopic analysis in conjunction with single-crystal X-ray diffraction studies. Some of the iron complexes show good activities in the selective dimerization of ethylene upon treat-

ment with MAO or MMAO, while the cobalt complexes show higher activities than their iron analogues and lead to the formation of C₆ and C₈ oligomers. The nickel complexes display high catalytic activities toward ethylene oligomerization in the presence of Et₂AlCl and an auxiliary ligand (PPh₃).

(© Wiley-VCH Verlag GmbH & Co. KGaA, 69451 Weinheim, Germany, 2007)

Introduction

Ethylene oligomerization is an important catalytic process for the production of linear α -olefins as basic chemicals.^[1] The catalysts currently used in industrial processes include alkylaluminum compounds, a combination of alkylaluminum compounds and early transition metal complexes, nickel(II) complexes,^[1a] and monoanionic [P,O] nickel-based catalysts (SHOP).^[2] In the past decade, research on late transition metal complexes as catalysts for ethylene oligomerization and polymerization has attracted considerable attraction in both academic and industrial circles due to the possibility of their forming highly active and selective catalysts.^[3–5] This was stimulated by the pioneering work by Brookhart's group,^[6] who discovered that cationic α -diiminonickel complexes are effective catalysts for ethylene oligomerization and polymerization. Since this initial investigation of tetracoordinate nickel complexes, more attention has been paid recently to pentacoordinate complexes of nickel incorporating tridentate ligands such as N[^]N[^]N[^]O,^[7] N[^]P[^]N[^],^[8] P[^]N[^]N[^],^[9] P[^]N[^]P[^],^[9a] and N[^]N[^]N[^],^[10–15] as well as their iron and cobalt analogues.

The discovery of highly active iron- and cobalt-based olefin polymerization catalysts was made possible by the design of bis(imino)pyridines as tridentate ligands by the Brookhart and Gibson groups,^[16] who carried out detailed investigations of metal complexes bearing bis(imino)pyridine ligands by modifying the substituents on the aryl ring linked to the imino group and checking their influence on

the catalytic activity and the resulting oligomerization or polymerization products.^[4] Extensive research into alternative models of iron and cobalt complexes ligated with new types of tridentate N₃ ligands did not result in highly active precursors for ethylene oligomerization or polymerization.^[17] Nevertheless, tridentate N₃ ligands are still of great interest for the preparation of late transition metal complexes as catalysts for ethylene oligomerization and polymerization^[10–15,17–20] as the selective synthesis of short ethylene oligomers, particularly α -olefins, is of industrial importance.

The variation of catalyst models by designing new organic compounds that can be used as tridentate ligands has been targeted by our group for the production of highly active catalysts of iron and cobalt,^[11,15,19,20] as well as nickel.^[11–14] Some of these complexes have shown promising catalytic activities toward ethylene oligomerization and polymerization, such as highly active iron catalysts bearing 2-imino-1,10-phenanthrolines^[19] and 2-(2-benzimidazolyl)-2-[1-(arylimino)ethyl]pyridines^[15b] along with bimetallic iron complexes bearing 2-methyl-2,4-bis(6-iminopyridin-2-yl)-1*H*-1,5-benzodiazepines;^[15a] their cobalt analogues also showed good activities.^[15a,15b,20] Similarly to the bis(imino)pyridine catalytic systems,^[4] we found that the above iron-based catalysts are generally more active than their cobalt analogues, although the exceptional cobalt complexes ligated by 2,9-bis(imino)-1,10-phenanthrolines showed better activity than their iron analogues.^[11] Moreover, all the corresponding nickel complexes showed good catalytic activity for ethylene oligomerization,^[11,12,14a] as did our more recent nickel complexes bearing 2-(benzimidazol-2-yl)-1,10-phenanthrolines.^[13]

Along with the decisive influence of the ligands, especially the steric and electronic effects of substituents, on the

[a] Key Laboratory of Engineering Plastics and Beijing National Laboratory for Molecular Sciences, Institute of Chemistry, Chinese Academy of Sciences, Beijing 100080, China
Fax: +86-10-6261-8239
E-mail: whsun@iccas.ac.cn

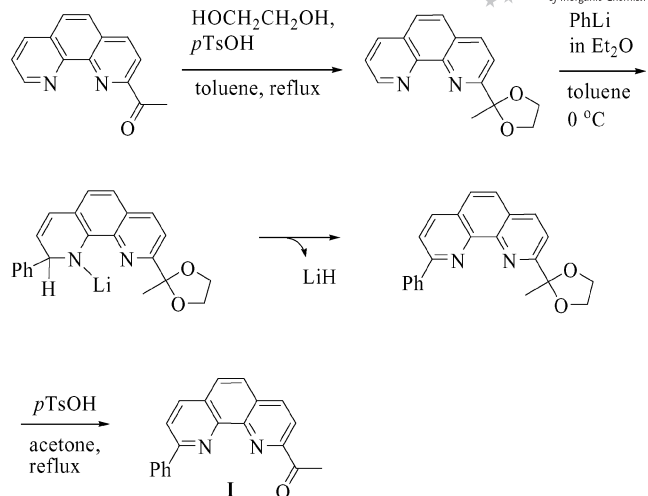
catalytic activities and products, the nature of the metal also greatly affects catalytic behavior. Metal complexes containing 2-imino-1,10-phenanthrolines generally show good to high catalytic activities for ethylene oligomerization and polymerization.^[12,19,20] A high steric bulk of the ligands was recognized to be critical for a high catalytic activity of diiminonickel complexes for ethylene polymerization,^[6] whereas, in comparison with 2-imino-1,10-phenanthrolyl metal complexes,^[12,19,20] the additional imino group in metal complexes bearing 2,9-diimino-1,10-phenanthrolines^[11] has a negative effect as the additional imino group is assumed to coordinate to the active species, which results in a deactivated species. In order to check the effect of steric hindrance, 2-imino-9-phenyl-1,10-phenanthroline complexes have been targeted as precursors for ethylene oligomerization.

Herein we report the synthesis of 2-acetyl- and 2-benzoyl-9-phenyl-1,10-phenanthrolines and their subsequent transformation into 2-imino-9-phenyl-1,10-phenanthrolines for use as ligands. These compounds keep the same coordinative framework as 2-imino-1,10-phenanthrolines but with an additional phenyl group at the 9-position. Their late transition metal (Fe, Co, and Ni) complexes are synthesized and characterized and the catalytic properties of these complexes for ethylene oligomerization are evaluated under various reaction conditions. The effects of ligand environment and reaction conditions on the activity and the distribution of oligomers obtained are investigated systematically.

Results and Discussion

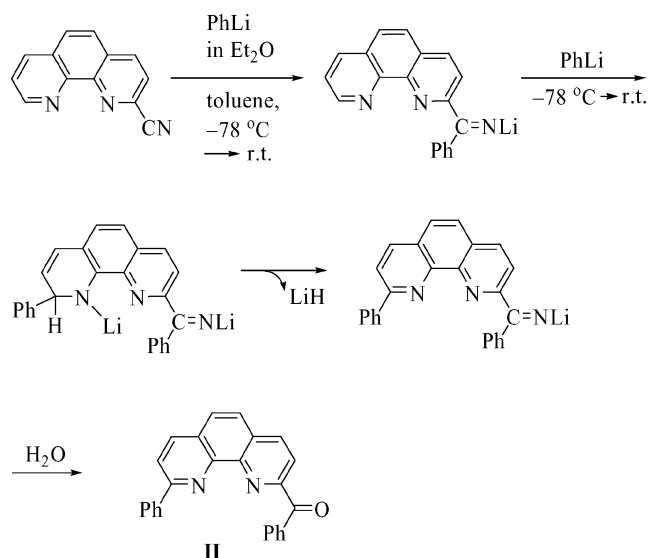
Preparation of Ketones I and II

2-Cyano-1,10-phenanthroline and 2-acetyl-1,10-phenanthroline were prepared according to the literature procedures.^[19a,21] 2-Acetyl-9-phenyl-1,10-phenanthroline (ketone I) was synthesized by attaching a phenyl group at the phenanthroline ring using 2-acetyl-1,10-phenanthroline as the starting material (Scheme 1). The carbonyl group of 2-acetyl-1,10-phenanthroline was first protected with ethylene glycol and the 2-(2-methyl-1,3-dioxolan-2-yl)-1,10-phenanthroline formed in this condensation reaction was purified on an alumina column.^[22] A solution of 1.7 equivalents of phenyllithium in diethyl ether was added dropwise to a suspension of 2-(2-methyl-1,3-dioxolan-2-yl)-1,10-phenanthroline in toluene under nitrogen at low temperature (0 °C) and the reaction mixture was maintained for an additional 3 h at 0 °C.^[23] This procedure gave 2-(2-methyl-1,3-dioxolan-2-yl)-9-phenyl-1,10-phenanthroline by elimination of lithium hydride.^[24] 2-(2-Methyl-1,3-dioxolan-2-yl)-9-phenyl-1,10-phenanthroline was purified as a yellow oil on a silica column and then refluxed in acetone in the presence of *p*-toluenesulfonic acid to cleave the 1,3-dioxolane moiety. The desired product (2-acetyl-9-phenyl-1,10-phenanthroline) precipitated from the solution and was obtained by filtration as a pale-yellow solid.



Scheme 1. Synthesis of ketone I.

2-Benzoyl-9-phenyl-1,10-phenanthroline (ketone II) was prepared in a one-step reaction between 2-cyano-1,10-phenanthroline and three equivalents of phenyllithium (Scheme 2). Thus, a solution of phenyllithium in diethyl ether was added dropwise to a suspension of 2-cyano-1,10-phenanthroline in toluene at −78 °C, then the mixture was slowly warmed to room temperature and stirred overnight. The reaction proceeds by initial addition of phenyllithium to the nitrile group^[25] followed by a Ziegler alkylation.^[24] Subsequent hydrolysis gave the benzoyl-substituted product. The resultant mixture was extracted with dichloromethane and the organic phase was purified on a silica column. The desired compound (2-benzoyl-9-phenyl-1,10-phenanthroline) was obtained as a slightly yellow solid in acceptable yield.



Scheme 2. Synthesis of ketone II.

Synthesis and Characterization of Ligands 1–6 and Complexes 1a–6a, 1b–6b, and 1c–6c

The 2-imino-9-phenyl-1,10-phenanthroline ligands **1–6** were prepared by condensing ketones **I** or **II** with the corresponding substituted anilines in the presence of *p*-toluenesulfonic acid in toluene or tetraethyl silicate (Scheme 3). The ligands were obtained in high yield and were characterized by IR, ^1H , and ^{13}C NMR spectroscopy as well as elemental analysis. The iron complexes **1a–6a** were readily prepared by mixing the corresponding ligand with one equivalent of $\text{FeCl}_2 \cdot 4\text{H}_2\text{O}$ in thf at room temperature under nitrogen (Scheme 3). The resulting complexes precipitated from the reaction solution and were separated as air-stable green or brown solids. Similarly, the cobalt complexes **1b–6b** and nickel complexes **1c–6c** were synthesized by treating the corresponding ligand with one equivalent of CoCl_2 or $\text{NiCl}_2 \cdot 6\text{H}_2\text{O}$ in anhydrous ethanol at room temperature. The methyl ketimine cobalt complexes **1b–3b** were obtained as green powders, whereas the phenyl ketimine complexes **4b–6b** were red-brown. The corresponding nickel complexes **1c–6c** were obtained as orange or yellow powders. All complexes were well characterized by FT-IR spectroscopy and elemental analysis. A comparison of the IR spectra of the complexes and their corresponding ligands shows that the C=N stretching vibrations of the iron, cobalt, and nickel complexes are shifted to lower wavenumber and their peak intensities greatly reduced, thereby indicating a coordinative interaction between the imino nitrogen atom and the central metal. Some samples for elemental analysis were prepared as crystals, therefore the analytical results show the incorporation of solvent molecules. The structures of ligand

2, iron complex **2a**, cobalt complexes **1b**, **4b**, and **6b**, and nickel complexes **1c** and **5c** in the solid state were confirmed by single-crystal X-ray diffraction analysis.

Crystal Structures

Single crystals of ligand **2** suitable for X-ray diffraction analysis were grown by recrystallization from a dichloromethane/hexane (1:5, v/v) solution. The molecular structure is shown in Figure 1. The imino nitrogen atom is disposed *trans* to the phenanthroline nitrogen atoms with a typical C=N double bond length of 1.270(2) Å. The phenyl ring on C1 is nearly coplanar with the plane of the phenanthroline moiety (dihedral angle: 6.2°), whereas the aryl ring on the imino nitrogen atom is approximately perpendicular to the plane of the phenanthroline moiety and the phenyl plane on C1 (dihedral angles: 92.1 and 89.6°, respectively).

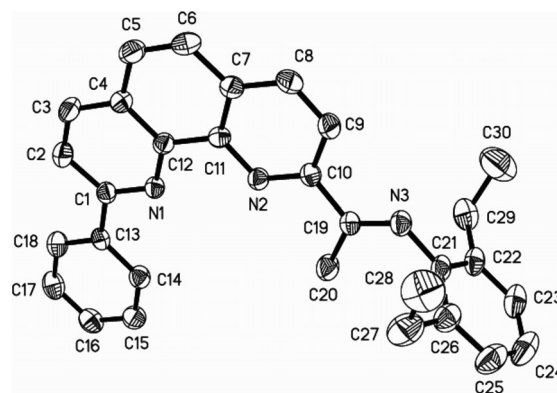
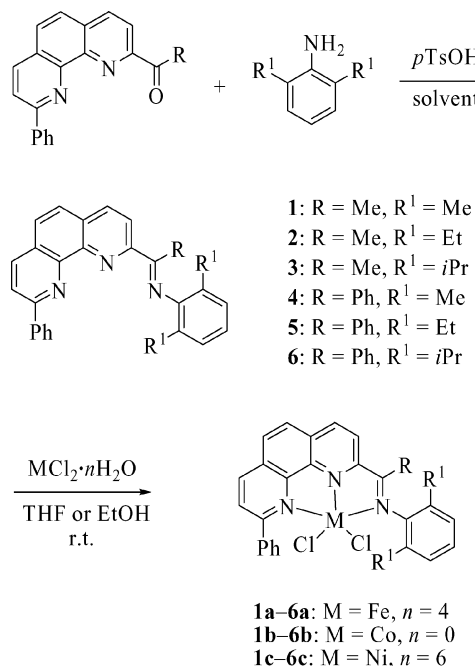


Figure 1. Molecular structure of ligand **2** with all hydrogen atoms omitted for clarity. Selected bond lengths [Å] and bond angles [°]: N1–C1 1.330(2), N1–C12 1.355(3), N2–C11 1.356(3), N2–C10 1.327(2), N3–C19 1.270(2), N3–C21 1.422(3); C19–N3–C21 121.62(2), N3–C19–C10 117.6(2), N3–C19–C20 125.0(2).



Scheme 3. Synthesis of ligands **1–6** and complexes **1a–6a**, **1b–6b**, and **1c–6c**.

Single crystals of complex **2a** suitable for X-ray diffraction analysis were obtained by slow diffusion of diethyl ether into its methanol solution under nitrogen. The asymmetric unit of complex **2a** contains the halves of two independent molecules, as shown in Figure 2. The coordination geometry around the iron center can be described as a distorted trigonal bipyramid in which N2 of the phenanthroline group and two chlorides form the equatorial plane. The two independent molecules have slightly different bond lengths and bond angles, as shown in Table 1. The iron center deviates slightly (0.0469 Å) from the equatorial plane in both molecules, and the phenyl ring on C1 or C1A and the plane of the phenanthroline moiety make the same dihedral angle (53.5°), which is very different from that in the corresponding ligand **2** (6.2°). The plane of the phenanthroline moiety is nearly perpendicular to the equatorial plane [86.8° in (a) and 88.4° in (b)]. The dihedral angles between the phenyl ring on C1 or C1A and the equatorial plane are also the same (139.1°) for the two molecules, while the angles between the aryl ring on the imino nitrogen atom and the

equatorial plane are very different [56.8° in (a) and 78.9° in (b)]. The Fe–N bond in the equatorial plane in each molecule is clearly shorter than the two axial Fe–N bonds, and the axial Fe–N(phenanthroline) bond is about 0.1 Å longer than the Fe–N(imino) bond. The phenyl group on C1 results in a longer Fe–N1 bond length [av. 2.392(3) Å] than that of a related 2-acetyl-1,10-phenanthroline complex [2.271(3) Å].^[19a] The two Fe–Cl bond lengths differ by about 0.1 Å. Although the two imino C=N bonds are slightly different [1.293(5) Å in (a) and 1.271(5) Å in (b)], they are both typical of an imino C=N double bond. The C=N bond length in molecule (b) is almost identical to that in ligand **2** [1.270(2) Å].

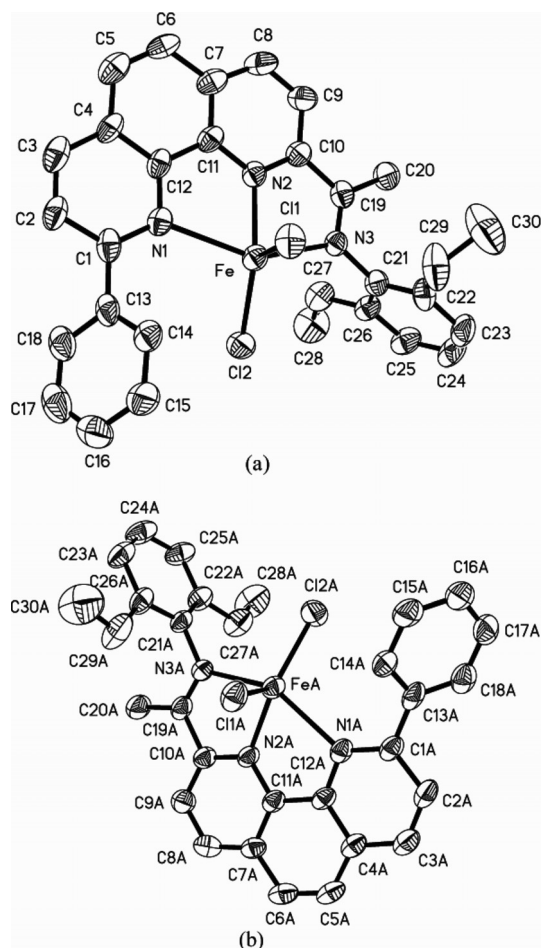


Figure 2. Molecular structure of complex **2a** showing the two crystallographically independent molecules of the asymmetric unit. Water molecules and all hydrogen atoms have been omitted for clarity.

Single crystals of cobalt complexes **1b**, **4b**, and **6b** were grown by slow diffusion of hexane into their solutions in dichloromethane. Their molecular structures are shown in Figures 3, 4, and 5, respectively, and selected bond lengths and angles are collected in Table 2. The coordination geometry around the cobalt center in these complexes can be described as a distorted trigonal bipyramid with N2 of the phenanthroline moiety and two chlorides forming the equatorial plane.

Table 1. Selected bond lengths [Å] and angles [°] for complex **2a**.

Fe–N1	2.391(3)	FeA–N1A	2.393(3)
Fe–N2	2.101(3)	FeA–N2A	2.104(3)
Fe–N3	2.298(3)	FeA–N3A	2.283(3)
Fe–Cl1	2.3405(1)	FeA–Cl1A	2.3456(1)
Fe–Cl2	2.2492(1)	FeA–Cl2A	2.2469(1)
N3–C19	1.293(5)	N3A–C19A	1.271(5)
N2–Fe–N1	73.77(1)	N2A–FeA–N1A	73.18(1)
N2–Fe–N3	73.18(1)	N2A–FeA–N3A	72.89(1)
N1–Fe–N3	145.86(1)	N1A–FeA–N3A	144.89(1)
N1–Fe–Cl1	93.70(8)	N1A–FeA–Cl1A	94.32(8)
N2–Fe–Cl1	98.23(9)	N2A–FeA–Cl1A	98.71(9)
N3–Fe–Cl1	99.19(8)	N3A–FeA–Cl1A	99.43(9)
N1–Fe–Cl2	104.73(9)	N1A–FeA–Cl2A	105.71(9)
N2–Fe–Cl2	141.53(9)	N2A–FeA–Cl2A	143.73(9)
N3–Fe–Cl2	95.87(9)	N3A–FeA–Cl2A	96.35(9)
Cl1–Fe–Cl2	120.09(5)	Cl1A–FeA–Cl2A	117.38(5)

The cobalt atom in complex **1b** deviates slightly (–0.0517 Å) from the equatorial plane composed by N2, Cl1, and Cl2 and the axial Co–N bonds form an angle of 149.22(1)° (N1–Co–N3). The phenyl ring on C1 and the plane of the phenanthroline moiety form a dihedral angle of 41.0°, and the plane of the phenanthroline moiety is almost perpendicular to the equatorial plane (dihedral angle: 93.2°). The dihedral angles between the phenyl ring on C1 and the equatorial plane and the aryl ring on the imino nitrogen atom and the equatorial plane are 134.0° and 133.7°, respectively. The two axial Co–N distances [2.313(4) and 2.279(4) Å] are much longer than the Co–N bond [2.035(4) Å] in the equatorial plane and the two Co–Cl linkages differ by 0.06 Å. The imino N3–C19 bond length is 1.289(6) Å, which is typical of a C=N double bond.

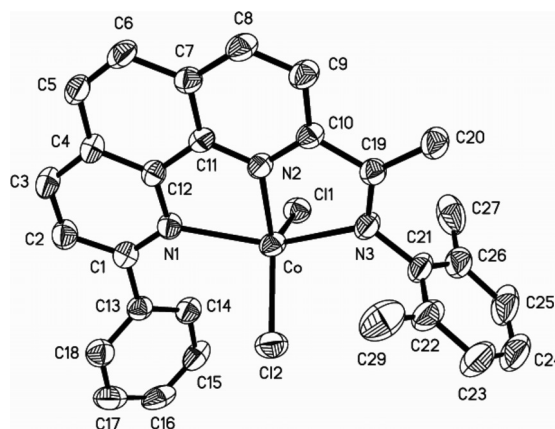


Figure 3. Molecular structure of complex **1b**. Water molecules and all hydrogen atoms have been omitted for clarity.

The central cobalt atom in the phenyl ketimine complex **4b** also deviates slightly (0.0196 Å) from the equatorial plane containing N2, Cl1, and Cl2. The bond lengths and angles around the cobalt center are very similar to those in **1b**, although the phenyl ring on C1 and the plane of the phenanthroline moiety make a dihedral angle (16.4°) that is very different from that in **1b** (41.0°). The phenyl ring on

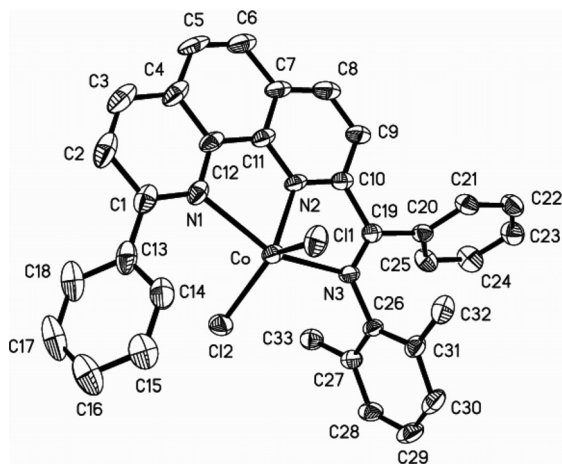


Figure 4. Molecular structure of complex **4b** showing one CH_2Cl_2 molecule. All hydrogen atoms have been omitted for clarity.

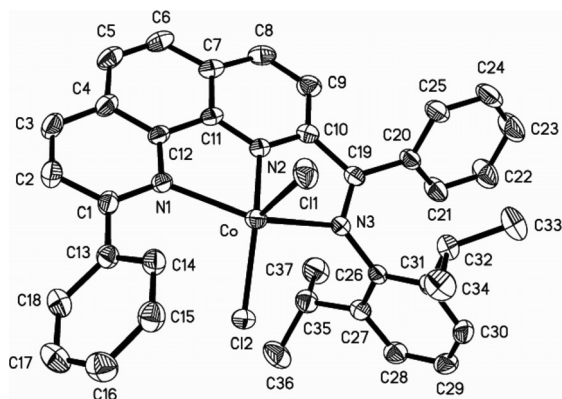


Figure 5. Molecular structure of complex **6b** showing one CH_2Cl_2 molecule. All hydrogen atoms have been omitted for clarity.

C1, the plane of the phenanthroline moiety, the phenyl ring on the imino carbon atom, and the aryl ring on the imino nitrogen atom are all approximately perpendicular to the equatorial plane, with dihedral angles of 80.1° , 88.9° , 91.5° , and 86.0° , respectively.

The central cobalt atom in the phenyl ketimine complex **6b**, which contains bulkier isopropyl groups at the *ortho* positions of the aryl ring at the imino nitrogen atom, deviates slightly more (0.1829 \AA) from the equatorial plane containing N2, C11, and C12 than in the other complexes. This complex also has a smaller N2–Co–C11 bond angle [$97.27(8)^\circ$] and larger N2–Co–C12 bond angle [$140.69(8)^\circ$]. The two axial Co–N bonds also make a slightly smaller angle of $143.99(9)^\circ$ (N1–Co–N3). In contrast to the other complexes, the phenyl ring on C1 is nearly coplanar to the plane of the phenanthroline moiety, with a dihedral angle of 3.3° that is much smaller than in other analogues and even smaller than in ligand **2** (6.2°). The dihedral angles between the phenyl ring on C1, the plane of the phenanthroline moiety, the phenyl ring on the imino carbon, and the aryl ring on the imino nitrogen and the equatorial plane [82.8° , 80.4° , 88.9° , and 89.2° , respectively] are similar to those in **4b**. The axial Co–N1(phenanthroline) bond in **6b** is 0.19 \AA shorter than the Co–N3(imino) bond, which is very different from the situation in other cobalt analogues (about 0.04 \AA in **1b** and **4b**). One possible reason for this is that the bulkier isopropyl groups at the *ortho* positions of the aryl ring bound to the imino nitrogen take up more space and lead to a shortening of the Co–N1 bond [$2.180(2) \text{ \AA}$] and a lengthening of the Co–N3 bond [$2.372(2) \text{ \AA}$]. This steric effect also leads to a shortening of the imino N3–C19 bond [$1.255(4) \text{ \AA}$].

Single crystals of nickel complexes **1c** and **5c** were obtained by layering hexane on their corresponding dichloromethane solutions. X-ray diffraction analysis revealed that they display a distorted trigonal bipyramidal geometry in which the central nickel atom is coordinated to three nitrogen atoms from the ligand and two halides. Similar to their iron and cobalt analogues, one nitrogen atom (N2) of the phenanthroline group and two chlorides compose the equatorial plane; the imino nitrogen (N3) and another nitrogen (N1) of the phenanthroline group occupy the two axial coordination sites. Their molecular structures are shown in Figures 6 and 7, respectively, and selected bond lengths and angles are collected in Table 2.

Table 2. Selected bond lengths [\AA] and bond angles [$^\circ$] in complexes **1b**, **1c**, **4b**, **5c**, and **6b**.

	1b (M = Co)	1c (M = Ni)	4b (M = Co)	5c (M = Ni)	6b (M = Co)
M–N1	2.313(4)	2.300(7)	2.299(3)	2.219(3)	2.180(2)
M–N2	2.035(4)	1.962(6)	2.034(3)	1.970(4)	2.012(2)
M–N3	2.279(4)	2.238(6)	2.257(3)	2.220(3)	2.372(2)
M–Cl1	2.2923(2)	2.274(3)	2.2745(1)	2.2988(1)	2.2192(1)
M–Cl2	2.2357(2)	2.217(3)	2.2404(1)	2.2234(1)	2.1917(9)
N3–C19	1.289(6)	1.275(9)	1.278(4)	1.276(5)	1.255(4)
N1–M–N2	76.16(15)	78.4(3)	76.64(12)	78.32(1)	77.62(1)
N2–M–N3	74.00(15)	76.0(3)	74.01(1)	75.40(1)	70.50(9)
N1–M–N3	149.22(1)	154.1(2)	149.77(1)	152.86(1)	143.99(9)
N1–M–Cl1	97.95(11)	95.46(2)	94.07(8)	91.79(1)	103.79(7)
N1–M–Cl2	99.72(1)	92.28(2)	96.22(8)	98.16(1)	103.95(7)
N2–M–Cl1	104.94(1)	101.4(2)	100.88(8)	99.41(1)	97.27(8)
N2–M–Cl2	133.77(1)	120.9(2)	131.09(8)	129.52(1)	140.69(8)
N3–M–Cl1	96.80(1)	93.11(2)	98.37(8)	99.04(1)	96.55(7)
N3–M–Cl2	95.48(1)	97.66(2)	97.55(8)	93.33(1)	90.89(7)
Cl1–M–Cl2	121.12(6)	137.71(1)	128.01(5)	131.07(6)	119.62(4)

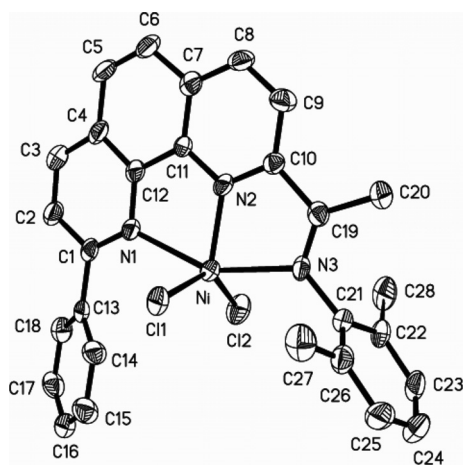


Figure 6. Molecular structure of complex **1c** showing one CH_2Cl_2 molecule. All hydrogen atoms have been omitted for clarity.

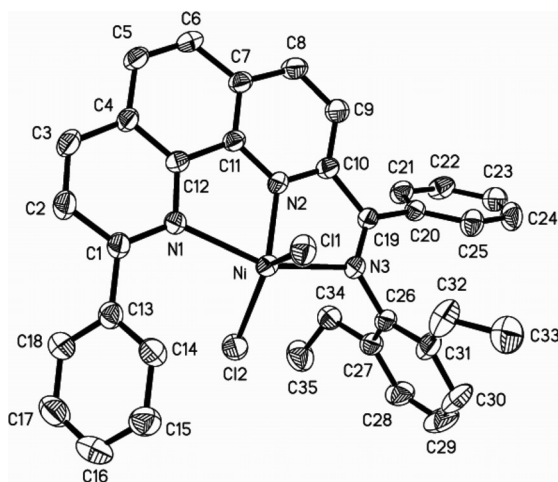


Figure 7. Molecular structure of complex **6b** showing two CH_2Cl_2 molecules. All hydrogen atoms have been omitted for clarity.

The central nickel atom in **1c** deviates by 0.0128 \AA from the equatorial plane containing N2, Cl1, and Cl2 and the two axial Ni–Cl bonds make an axial angle (N1–Ni–N3) of $154.1(2)^\circ$. Both the equatorial plane and the plane of the phenyl group on the imino nitrogen are almost perpendicular to the plane of the phenanthroline moiety (dihedral angles of 84.8° and 87.8° , respectively). The plane of the pendant phenyl group on C1 makes a dihedral angle of 33.6° with the plane of the phenanthroline moiety and 51.2° with the equatorial plane. Similarly to a related phenanthrolynickel complex, the Ni–N bond in the equatorial plane is clearly shorter than the axial Ni–N bonds, although the presence of a phenyl group on C1 leads to an elongation of the Ni–N1 bond [$2.300(7) \text{ \AA}$ vs. $2.157(3) \text{ \AA}$];^[12] the two Ni–Cl bond lengths are essentially identical. Despite showing typical character of a C=N double bond, the imino N3–C19 bond [$1.275(9) \text{ \AA}$] is slightly shorter than that in a related phenanthrolynickel complex [$1.284(4) \text{ \AA}$];^[12] whereas much larger Cl1–Ni–Cl2 [$137.71(1)^\circ$] and smaller N2–Ni–Cl1 [$120.9(2)^\circ$] bond angles are observed after addition of a phenyl group at the 9-position of phenanthroline

[$110.62(4)^\circ$ and $153.12(8)^\circ$, respectively, in the related nickel complex].^[12]

Despite several similarities with **1c**, complex **5c** also has its own structural characteristics due to the presence of a phenyl group at the imino carbon instead of a methyl group. Thus, the central nickel atom deviates 0.0102 \AA from the equatorial plane containing N2, Cl1, and Cl2, and the introduced phenyl group forms a dihedral angle of 5.7° with the plane of the phenanthroline moiety and is almost perpendicular to the equatorial plane (dihedral angle of 82.2°). The equatorial plane is still almost perpendicular to the plane of the phenanthroline moiety (dihedral angle of 87.5°), whereas the dihedral angle between the plane of the phenyl group on the imino nitrogen and the plane of the phenanthroline moiety decreases significantly to 7.2° . The plane of the pendant phenyl group on C1 makes a decreased dihedral angle of 8.0° with the plane of the phenanthroline moiety and an increased dihedral angle of 79.9° with the equatorial plane. All bond lengths and angles in **5c** are similar to those in **1c**.

Ethylene Oligomerization

Ethylene Oligomerization with Iron Complexes 1a–6a

The iron(II) complexes **1a–6a** were first investigated as ethylene oligomerization catalysts at 1 atm of ethylene pressure (Table 3), although the results were not satisfactory as almost no absorption of ethylene was observed with diethylaluminum chloride as co-catalyst. Activation with methylaluminumoxane (MAO) gave a low catalytic activity for methyl-substituted complexes **1a** and **4a**, although ethyl-substituted complexes **2a** and **5a** were found to be less active and isopropyl-substituted complexes **3a** and **6a** completely inactive. Modified methylaluminumoxane (MMAO) was found to be a more effective co-catalyst than MAO with a similar effect of the ligand environment on the catalytic activity. Thus, for complexes bearing the same substituents on the aryl ring of the imino nitrogen, phenyl ketimine (R = Ph) complexes **4a–6a** showed a relatively higher catalytic activity than the corresponding methyl ketimine (R = Me) complexes **1a–3a**. Complex **4a** exhibited the highest activity of $2.64 \times 10^5 \text{ g mol}^{-1}(\text{Fe})\text{h}^{-1}$, with 1-butene as the main product. Under the same reaction conditions, the variation of R¹ on the aryl ring of the imino nitrogen was found to have a strong influence on the catalytic activity. Thus, increasing the bulkiness of R¹ in both methyl and phenyl ketimine complexes caused the catalytic activity to decrease dramatically (methyl > ethyl > isopropyl), and in all cases essentially only dimerization was achieved, with a high selectivity for 1-butene.

The iron(II) complexes **1a–6a** were studied for ethylene oligomerization at 10 atm of ethylene pressure in the presence of MAO or MMAO; much higher catalytic activities were observed than those obtained at 1 atm (Table 3). With MAO as a co-catalyst the highest activity of $1.94 \times 10^6 \text{ g mol}^{-1}(\text{Fe})\text{h}^{-1}$ was obtained with complex **4a**. In general, however, under similar conditions, these complexes

Table 3. Ethylene oligomerization with complexes **1a–6a**.^[a]

Entry	Cat.	Co-cat.	<i>P</i> [atm] ^[b]	<i>T</i> [°C] ^[c]	Activity ^[d]	% Oligomer distribution ^[e]		% Selectivity for 1-C ₄ ^[e]
						C ₄ /ΣC	C ₆ /ΣC	
1	1a	MAO	1	20	0.259	100	–	96.1
2	2a	MAO	1	20	0.059	100	–	100
3	3a	MAO	1	20	–	–	–	–
4	4a	MAO	1	20	0.295	100	–	100
5	5a	MAO	1	20	0.052	100	–	100
6	6a	MAO	1	20	–	–	–	–
7	1a	MMAO	1	20	4.78	100	–	100
8	2a	MMAO	1	20	1.63	100	–	100
9	3a	MMAO	1	20	0.199	100	–	100
10	4a	MMAO	1	20	26.4	100	–	100
11	5a	MMAO	1	20	5.13	100	–	100
12	6a	MMAO	1	20	0.275	100	–	100
13	1a	MAO	10	40	40.8	99.2	0.8	99.8
14	2a	MAO	10	40	29.1	98.7	1.3	99.8
15	3a	MAO	10	40	0.621	100	–	100
16	4a	MAO	10	40	194	99.2	0.8	99.9
17	5a	MAO	10	40	51.6	98.6	1.4	100
18	6a	MAO	10	40	0.409	100	–	100
19	1a	MMAO	10	40	269	99.4	0.6	100
20	2a	MMAO	10	40	47.9	100	–	100
21	3a	MMAO	10	40	1.90	100	–	100
22	4a	MMAO	10	40	211	99.1	0.9	100
23	5a	MMAO	10	40	54.3	98.7	1.3	100
24	6a	MMAO	10	40	0.465	100	–	100

[a] General conditions: cat.: 5 μmol; Al/Fe: 500; solvent (toluene): 30 mL for 1 atm and 100 mL for 10 atm; reaction time: 30 min. [b] Ethylene pressure. [c] Reaction temperature. [d] 10⁴ g mol^{−1}(Fe)h^{−1}. [e] Weight percentage determined by GC.

were found to be much less active than the corresponding 2-imino-1,10-phenanthroline complexes,^[19] probably due to the presence of a phenyl group at the 9-position of the 1,10-phenanthroline ligand, which hinders the insertion of ethylene. MMAO was found to be more effective than MAO at 10 atm of ethylene pressure, and the methyl-substituted complexes **1a** [2.69×10^6 g mol^{−1}(Fe)h^{−1}] and **4a** [2.11×10^6 g mol^{−1}(Fe)h^{−1}] displayed the highest activity. The isopropyl-substituted complexes **3a** and **6a** always showed lower catalytic activity, probably because the bulkier isopropyl groups at the *ortho* positions of the aryl ring at the imino nitrogen affect the active species by preventing the coordination of an ethylene molecule at the metal center. A similar trend to that obtained at 1 atm as regards the effect of ligand environment on the catalytic activities and catalytic products was obtained for both the MAO and MMAO catalytic systems.

Ethylene Oligomerization with Cobalt Complexes **1b–6b**

Complex **5b** was studied as a model for ethylene oligomerization under varying conditions at 1 atm of ethylene pressure (Table 4). No catalytic activity was observed with diethylaluminum chloride (Al/Co = 100 or 200) as co-catalyst at 20 °C, whereas in the presence of MAO or MMAO (Al/Co = 500) the catalytic activity increased remarkably and the products mainly consisted of butene and hexene, with a high selectivity for 1-butene (>96%). The catalytic system **5b**/MAO showed a higher activity than **5b**/MMAO, although both gave a similar distribution of oligomers and a similar selectivity for 1-butene (entries 1 and 4, Table 4). MAO was therefore chosen as a co-catalyst during the sub-

sequent investigations at 1 and 10 atm of ethylene pressure. The **5b**/MAO system showed the lowest activity, with a butene content in the oligomeric products of more than 90%, at an Al/Co molar ratio of 100 (entry 2, Table 4). Increasing the Al/Co molar ratio in the range 200–2000 led to an increase in the activity to 6.42×10^5 g mol^{−1}(Co)h^{−1} at a Al/Co molar ratio of 500 and then a gradual decrease. The distribution of oligomers and the selectivity for 1-butene hardly changed.

The reaction temperature was found to have a remarkable influence on the catalytic activity and the distribution of oligomers. The highest activity was achieved at 20 °C and a slightly lower activity was obtained, although with a higher amount of butene produced (91.0%), at lower temperature (0 °C; entry 8, Table 4). An elevated reaction temperature also resulted in a decrease of the catalytic activity and butene content; for instance, **5b**/MAO showed an activity of 8.74×10^4 g mol^{−1}(Co)h^{−1} with a 72.5% butene content at 80 °C (entry 11, Table 4). No significant difference was observed between methyl- and ethyl-substituted complexes for both methyl and phenyl ketimine complexes. However, the isopropyl-substituted complexes **3b** and **6b** displayed lower catalytic activities and gave a smaller amount of butene and higher amount of hexene than the corresponding methyl- or ethyl-substituted complexes. In contrast to bis(imino)pyridine,^[4] 2-benzimidazolyl-6-iminopyridine,^[15b] 2-quinoxalyl-6-iminopyridine,^[15c] and 2-imino-1,10-phenanthroline systems,^[19,20] these cobalt complexes display much higher catalytic activities than their corresponding iron analogues under similar reaction conditions.

Table 4. Ethylene oligomerization with complexes **1b–6b**.^[a]

Entry	Cat.	<i>P</i> [atm] ^[b]	Al/Co	<i>T</i> [°C] ^[c]	Activity ^[d]	% Oligomer distribution ^[e]			% Selectivity for 1-C ₄ ^[e]
						C ₄ /ΣC	C ₆ /ΣC	≥ C ₈ /ΣC	
1 ^[f]	5b	1	500	20	5.93	77.1	16.2	6.7	96.1
2	5b	1	100	20	0.76	90.7	5.9	3.4	98.0
3	5b	1	200	20	2.33	86.3	10.6	3.1	97.0
4	5b	1	500	20	6.42	78.5	15.2	6.3	96.7
5	5b	1	1000	20	5.70	77.8	15.1	7.1	97.4
6	5b	1	1500	20	5.42	76.0	16.7	7.3	96.1
7	5b	1	2000	20	4.31	82.2	14.8	3.0	98.2
8	5b	1	500	0	3.64	91.0	7.6	1.4	98.4
9	5b	1	500	40	5.05	81.1	16.0	2.9	95.9
10	5b	1	500	60	1.41	72.4	19.2	8.4	97.2
11	5b	1	500	80	0.874	72.5	16.6	10.9	96.3
12	1b	1	500	20	6.85	94.3	5.7	–	97.0
13	2b	1	500	20	6.71	91.9	5.4	2.7	97.9
14	3b	1	500	20	5.23	80.0	16.5	3.5	95.4
15	4b	1	500	20	5.58	84.4	14.8	0.8	96.4
16	6b	1	500	20	2.85	55.2	28.1	16.7	94.3
17	1b	10	500	30	43.2	92.1	7.6	0.3	99.8
18	2b	10	500	30	40.6	95.7	4.0	0.3	99.7
19	3b	10	500	30	65.2	75.7	23.0	1.3	99.7
20	4b	10	500	30	49.0	84.5	13.4	2.1	99.8
21	5b	10	500	30	73.3	80.5	16.8	2.7	99.7
22	6b	10	500	30	28.0	46.7	34.0	19.3	100

[a] General conditions: cat.: 5 μmol; co-cat.: MAO; solvent (toluene): 30 mL for 1 atm and 100 mL for 10 atm; reaction time: 30 min. [b] Ethylene pressure. [c] Reaction temperature. [d] 10⁵ g mol^{−1}(Co)h^{−1}. [e] Weight percentage determined by GC. [f] Co-cat.: MMAO.

When the ethylene pressure was increased from 1 to 10 atm the catalytic activity of each complex increased greatly, with a very high selectivity for 1-butene. Complex **5b** was found to have the highest activity [7.33×10^6 g mol^{−1}(Co)h^{−1}; entry 21, Table 4]. For methyl ketimine complexes, methyl-substituted **1b** and ethyl-substituted **2b** showed comparable catalytic activities and a similar distribution of oligomers, whereas isopropyl-substituted **3b** showed a higher activity and gave a larger amount of hexene than **1b** or **2b**. A slightly higher amount of hexene was obtained for the corresponding phenyl ketimine complexes than with the methyl ketimine complexes. Complex **6b**, which contains bulkier isopropyl groups on the aryl ring of the imino nitrogen, was found to be slightly less active and produce a wider distribution of oligomers (C₄ to C₂₂, along with a small amount of polyethylene waxes) than **4b** or **5b** (entry 22, Table 4).

Ethylene Oligomerization with Nickel Complexes **1c–6c**

Complex **5c** was investigated for ethylene oligomerization in the presence of different co-catalysts at 1 atm of ethylene pressure. Unlike the nickel complexes ligated by other 1,10-phenanthroline derivatives,^[11–13] almost no catalytic activity was observed with **5c** in the presence of MAO. When MMAO was used as a co-catalyst, however, slightly better activity was obtained and only butene was generated, with a high selectivity for 1-butene (entry 3, Table 5). However, Et₂AlCl was found to be more effective as a co-catalyst for nickel complexes, although the selectivity for 1-butene was slightly lower. For example, at an Al/Ni molar ratio of 300, **5c**/Et₂AlCl showed an activity of 1.43×10^4 g mol^{−1}(Ni)h^{−1},

with a selectivity of 78.5% for 1-butene, at 1 atm of ethylene pressure (entry 5, Table 5).

The addition of PPh₃ as an auxiliary ligand to nickel-based catalytic systems has been demonstrated to improve catalytic activity and prolong catalyst lifetime,^[7a,12,26] although the mechanism is still not clear. However, in the presence of MAO, the addition of PPh₃ had no effect and the system still had no activity. For the catalytic system **5c**/MMAO, the addition of 10 equiv. of PPh₃ resulted in an increase in catalytic activity but a drastic decrease in the selectivity for 1-butene (entry 4, Table 5).

The effect of varying the amount of PPh₃ added on the catalytic activity and the selectivity for 1-butene was investigated with the catalytic system **5c**/Et₂AlCl at 1 atm of ethylene pressure. Addition of two equivalents of PPh₃ improved the catalytic activity to 9.63×10^4 g mol^{−1}(Ni)h^{−1}, with a small amount of hexene generated, whereas the selectivity for 1-butene decreased from 78.5% to 27.1% (entry 6, Table 5). Increasing the amount of PPh₃ (≤20) led to a further enhancement of catalytic activity and a further decrease of selectivity for 1-butene. The addition of 20 equivalents of PPh₃ gave the highest activity [6.82×10^5 g mol^{−1}(Ni)h^{−1}] and the lowest selectivity (8.5%; entry 10, Table 5). Further increasing the amount of PPh₃ to 30 equivalents reduced the catalytic activity and increased the selectivity for 1-butene.

The effect of reaction temperature on the catalytic activity was also studied in the presence of 10 equivalents of PPh₃. When keeping the other conditions constant, the optimum catalytic activity was obtained at 20 °C; both increasing and decreasing the reaction temperature led to a lower catalytic activity and higher selectivity for 1-butene.

Table 5. Ethylene oligomerization with complexes **1c–6c**.^[a]

Entry	Cat.	Equiv. of PPh ₃ ^[b]	<i>P</i> [atm] ^[c]	<i>T</i> [°C] ^[d]	<i>t</i> [min] ^[e]	Activity ^[f]	% Oligomer distribution ^[g]		% Selectivity for 1-C ₄ ^[g]
							C ₄ /ΣC	C ₆ /ΣC	
1 ^[h]	5c	–	1	20	30	–	–	–	–
2 ^[h]	5c	10	1	20	30	–	–	–	–
3 ^[i]	5c	–	1	20	30	0.048	100	–	92.8
4 ^[i]	5c	10	1	20	30	0.128	100	–	41.6
5	5c	–	1	20	30	0.143	100	–	78.5
6	5c	2	1	20	30	0.963	97.8	2.2	27.1
7	5c	5	1	20	30	2.29	98.1	1.9	24.0
8	5c	10	1	20	30	3.31	98.1	1.9	15.9
9	5c	10	1	20	60	3.71	96.5	3.5	3.5
10	5c	20	1	20	30	6.82	97.7	2.3	8.5
11	5c	30	1	20	30	2.75	98.8	1.2	27.2
12	5c	10	1	0	30	1.14	99.2	0.8	34.6
13	5c	10	1	0	60	1.91	98.4	1.6	16.3
14	5c	10	1	40	30	2.36	97.2	2.8	22.7
15	5c	10	1	60	30	1.58	95.4	4.6	20.2
16	1c	10	1	20	30	3.74	98.0	2.0	17.5
17	1c	10	1	20	60	3.49	96.7	3.3	4.3
18	2c	10	1	20	30	3.29	97.3	2.7	15.9
19	2c	10	1	20	60	4.67	97.0	3.0	5.8
20	3c	10	1	20	30	3.33	97.5	2.5	14.0
21	3c	10	1	20	60	3.68	96.1	3.9	3.2
22	4c	10	1	20	30	3.47	97.8	2.2	15.2
23	4c	10	1	20	60	4.71	95.7	4.3	2.8
24	6c	10	1	20	30	5.88	97.5	2.5	10.6
25	6c	10	1	20	60	3.89	96.4	3.6	6.6
26	5c	–	10	30	30	2.26	98.9	1.1	97.1
27	5c	10	10	30	30	5.87	100	–	93.0
28	5c	20	10	30	30	51.7	97.5	2.5	36.5
29	1c	20	10	30	30	36.8	98.1	1.9	36.2
30	2c	20	10	30	30	61.5	98.7	1.3	50.2
31	3c	20	10	30	30	39.6	98.9	1.1	63.4
32	4c	20	10	30	30	39.1	98.1	1.9	38.9
33	6c	20	10	30	30	57.7	98.4	1.6	34.9

[a] General conditions: cat.: 5 μmol; co-cat.: Et₂AlCl; Al/Ni: 300; solvent (toluene): 30 mL for 1 atm and 100 mL for 10 atm. [b] PPh₃ was added as an auxiliary ligand. [c] Ethylene pressure. [d] Reaction temperature. [e] Reaction time. [f] 10⁵ g mol^{−1}(Ni)h^{−1}. [g] Weight percentage determined by GC. [h] Co-cat.: MAO; Al/Ni: 500. [i] Co-cat.: MMAO; Al/Ni: 500.

In general, an induction time of 10–20 min is observed after the addition of PPh₃, and a lower temperature led to a longer induction time and catalyst lifetime. For instance, the catalytic activity of **5c** at 0 or 20 °C after 60 min was found to be higher than that after 30 min, although a lower selectivity for 1-butene was obtained with a slightly larger amount of hexene produced after 60 min, which indicates that the isomerization reaction of 1-butene to 2-butene takes place at the same time as the oligomerization reaction. Generally, phenyl ketimine complexes display slightly higher activities than methyl ketimine complexes bearing the same substituents on the aryl ring of the imino nitrogen. The catalytic properties of methyl ketimine complexes after 30 min were found to be not greatly affected by the substituents on the aryl ring of the imino nitrogen, and complexes **1c–3c** showed comparable catalytic activity and similar selectivity for 1-butene. However, when the reaction time was prolonged to 60 min a higher catalytic activity and slightly higher selectivity for 1-butene were achieved with ethyl-substituted **2c** than with methyl-substituted **1c** and isopropyl-substituted **3c**. For phenyl ketimine complexes, isopropyl-substituted **6c** showed the highest activity of

$5.88 \times 10^5 \text{ g mol}^{-1}(\text{Ni})\text{h}^{-1}$ after 30 min and methyl-substituted **4c** showed the highest activity of $4.71 \times 10^5 \text{ g mol}^{-1}(\text{Ni})\text{h}^{-1}$ after 60 min (entry 23 and 24, Table 5).

The catalytic activity and selectivity for 1-butene of **5c** increased to $2.26 \times 10^5 \text{ g mol}^{-1}(\text{Ni})\text{h}^{-1}$ and 97.1%, respectively (entry 26, Table 5) at 10 atm of ethylene pressure without PPh₃, whereas at 1 atm the catalytic activity and the selectivity for 1-butene did not change greatly when 10 equivalents of PPh₃ was introduced into the catalytic system (entry 27, Table 5), which means that both the PPh₃/Ni molar ratio and the concentration of PPh₃ in the reaction solution affect the catalytic properties. When the amount of PPh₃ was increased to 20 equivalents the catalytic activity of **5c** increased to $5.17 \times 10^6 \text{ g mol}^{-1}(\text{Ni})\text{h}^{-1}$, with a lower selectivity for 1-butene (36.5%; entry 28, Table 5). Five other nickel complexes were therefore also investigated in the presence of 20 equivalents of PPh₃ at 10 atm of ethylene pressure. A higher catalytic activity and selectivity for 1-butene was obtained for each complex than at 1 atm, and the highest activity of $6.15 \times 10^6 \text{ g mol}^{-1}(\text{Ni})\text{h}^{-1}$ was achieved with **2c**, with a selectivity of 50.2% for 1-butene.

In general, the selectivity for 1-butene increases with increasing ethylene pressure, probably due to a competition between chain transfer and chain isomerization, and a higher ethylene concentration thus favors the formation of 1-butene due to rapid chain transfer rather than chain isomerization.^[27]

Conclusions

A series of iron, cobalt, and nickel complexes bearing 2-imino-9-phenyl-1,10-phenanthroline ligands have been synthesized, characterized, and evaluated as catalyst precursors in ethylene oligomerization. Some iron complexes show good catalytic activities, with high selectivity for ethylene oligomerization [**1a**/MMAO: $2.69 \times 10^6 \text{ g mol}^{-1}(\text{Fe})\text{h}^{-1}$], upon treatment with MAO or MMAO. Unexpectedly, in contrast to previous results with other tridentate N_3 catalytic systems, the cobalt complexes generally show much higher activities and broader oligomer distributions than the corresponding iron analogues. The ligand environment and the reaction parameters play an important role in influencing both the catalytic activity and the oligomer distributions for iron and cobalt complexes. The highest activity of up to $7.33 \times 10^6 \text{ g mol}^{-1}(\text{Co})\text{h}^{-1}$ for ethylene oligomerization has been obtained with the catalytic system **5b**/MAO at 10 atm of ethylene pressure. Et_2AlCl is a more effective co-catalyst for nickel complexes, and the addition of PPh_3 significantly improves the catalytic activity and prolong the catalyst lifetime. The addition of 20 equiv. of PPh_3 leads to higher catalytic activities at 10 atm of ethylene pressure.

Experimental Section

General: All manipulations of air- and moisture-sensitive compounds were carried out under an atmosphere of nitrogen using standard Schlenk techniques. Melting points were measured with a digital electrothermal apparatus without calibration. IR spectra were recorded with a Perkin–Elmer FT-IR 2000 spectrometer for KBr discs in the range 4000–400 cm^{-1} . ^1H and ^{13}C NMR spectra were recorded with a Bruker DMX-300 or DMX-400 instrument with TMS as the internal standard. Elemental analyses were performed with a Flash EA1112 microanalyzer. GC analyses were performed with a Varian CP-3800 gas chromatograph equipped with a flame ionization detector and a 30-m (0.2-mm i.d., 0.25- μm film thickness) CP-Sil 5 CB capillary column. The yield of oligomers was calculated by referencing to the mass of solvent on the basis of the prerequisite that the mass of each fraction is approximately proportional to its integrated area in the GC trace.

Toluene, diethyl ether and thf were refluxed over sodium-benzophenone and distilled under nitrogen prior to use. Diethylaluminum chloride was purchased from Acros Chemicals. Methylaluminoxane (MAO, 1.46 M in toluene) and modified methylaluminoxane (MMAO-3A, 7% aluminum in heptane solution) were purchased from Akzo Corp (USA). All other chemicals were obtained commercially and used without further purification unless otherwise stated.

Synthesis of 2-Acetyl-9-phenyl-1,10-phenanthroline (**I**)

2-(2-Methyl-1,3-dioxolan-2-yl)-1,10-phenanthroline: A mixture of 2-acetyl-1,10-phenanthroline (2.230 g, 10.0 mmol), glycol (3.254 g,

52.4 mmol) and *p*-toluenesulfonic acid (206 mg) was refluxed in toluene (100 mL) for 18 h until no further formation of water was observed in a Dean–Stark trap. The solvent was then removed under reduced pressure and the residue was eluted with petroleum ether/ethyl acetate (1:2, v/v) on an alumina column. The second eluting fraction was collected and concentrated to give a slightly yellow solid in 50.0% yield (1.333 g). M.p. 119–121 °C. FT-IR (KBr disc): $\tilde{\nu}$ = 3054, 2993, 2980, 2938, 2900, 1619, 1589, 1552, 1505, 1490, 1476, 1445, 1391, 1376, 1256, 1232, 1204, 1147, 1129, 1106, 1029, 1009, 953, 855, 789, 752, 675 cm^{-1} . ^1H NMR (400 MHz, CDCl_3): δ = 9.24 (d, J = 4.4 Hz, 1 H, phen), 8.25 (d, J = 8.4 Hz, 1 H, phen), 8.22 (d, J = 8.4 Hz, 1 H, phen), 7.93 (d, J = 8.4 Hz, 1 H, phen), 7.77 (s, 2 H, phen), 7.61 (dd, J_1 = 8.0 Hz, J_2 = 4.4 Hz, 1 H, phen), 4.18 (t, J = 6.4 Hz, 2 H, CH_2), 4.01 (t, J = 6.4 Hz, 2 H, CH_2), 1.98 (s, 3 H, CH_3) ppm. ^{13}C NMR (100 MHz, CDCl_3): δ = 161.5, 150.5, 146.4, 145.8, 136.8, 136.0, 129.0, 128.1, 126.7, 126.3, 122.9, 119.5, 109.2, 65.2, 25.6 ppm. $\text{C}_{16}\text{H}_{14}\text{N}_2\text{O}_2$ (266.29): calcd. C 72.16, H 5.30, N 10.52; found C 72.18, H 5.23, N 11.00.

2-Acetyl-9-phenyl-1,10-phenanthroline (I**):** A phenyllithium solution was prepared by slowly adding a solution of bromobenzene (0.9 mL, 8.50 mmol) in diethyl ether (20 mL) to two equiv. of lithium (118 mg, 17.0 mmol) in diethyl ether (30 mL) at room temperature under nitrogen. The phenyllithium solution was then added dropwise to a suspension of 2-(2-methyl-1,3-dioxolan-2-yl)-1,10-phenanthroline (1.333 g, 5.00 mmol) in toluene (40 mL) at 0 °C and the initial yellow suspension turned dark brown. The resultant solution was stirred under nitrogen at 0 °C for an additional 3 h, then the reaction was quenched by slow addition of water (100 mL) and the mixture stirred. The yellow organic layer was separated and the aqueous layer was extracted several times with CH_2Cl_2 . The organic phases were combined and dried with anhydrous sodium sulfate. After evaporation of the solvent the residue was purified on a silica column to give the pure product as a yellow oil. This oil was dissolved in 50 mL of acetone containing *p*-toluenesulfonic acid (170 mg) as a catalyst and refluxed for 15 h. The desired product was precipitated from the solution and collected by filtration as a pale-yellow solid in 47.5% yield (710 mg). M.p. 184–186 °C. FT-IR (KBr disc): $\tilde{\nu}$ = 3103, 3026, 2916, 1694, 1633, 1620, 1597, 1565, 1537, 1495, 1367, 1285, 1219, 1190, 1120, 1034, 1011, 888, 817, 766, 741, 678, 566 cm^{-1} . ^1H NMR (300 MHz, CDCl_3): δ = 8.44 (d, J = 7.2 Hz, 2 H, Ph), 8.34 (d, J = 3.0 Hz, 2 H, phen), 8.30 (d, J = 8.4 Hz, 1 H, phen), 8.17 (d, J = 8.4 Hz, 1 H, phen), 7.88 (d, J = 8.7 Hz, 1 H, phen), 7.78 (d, J = 8.7 Hz, 1 H, phen), 7.59 (t, J = 7.2 Hz, 2 H, Ph), 7.50 (t, J = 7.2 Hz, 1 H, Ph), 3.14 (s, 3 H, COCH_3) ppm. ^{13}C NMR (75 MHz, CDCl_3): δ = 200.3, 156.6, 152.3, 145.4, 144.8, 138.5, 136.5, 130.4, 129.3, 128.4, 128.1, 127.3, 127.0, 125.3, 119.7, 119.6, 25.2 ppm. $\text{C}_{20}\text{H}_{14}\text{N}_2\text{O}$ (298.34): calcd. C 82.52, H 4.73, N 9.39; found C 80.00, H 4.77, N 9.36.

Synthesis of 2-Benzoyl-9-phenyl-1,10-phenanthroline (II**):** A phenyllithium solution was prepared by slowly adding a solution of bromobenzene (3.2 mL, 30.5 mmol) in diethyl ether (20 mL) to two equiv. of lithium (439 mg, 63.2 mmol) in diethyl ether (30 mL) at room temperature under nitrogen. This phenyllithium solution was then added dropwise to a suspension of 2-cyano-1,10-phenanthroline (2.053 g, 10.0 mmol) in toluene (50 mL) at –78 °C and the mixture was slowly warmed to room temperature. After stirring for 12 h at room temperature, the reaction was quenched by slow addition of water (100 mL) and the mixture stirred. The red organic layer was separated and the aqueous layer was extracted several times with CH_2Cl_2 . The organic phases were combined and dried with anhydrous sodium sulfate. After evaporation of the solvent the residue was purified on a silica column to give the pure product

as a yellow solid in 21.3% yield (1.245 g). M.p. 162–164 °C. FT-IR (KBr disc): $\tilde{\nu}$ = 3060, 3034, 1645, 1616, 1595, 1575, 1545, 1505, 1486, 1446, 1420, 1364, 1319, 1288, 1183, 1152, 1093, 1023, 944, 878, 865, 768, 716, 692 cm⁻¹. ¹H NMR (300 MHz, CDCl₃): δ = 8.93 (d, J = 7.2 Hz, 2 H, Ph), 8.55–8.39 (m, 4 H), 8.30 (d, J = 8.4 Hz, 1 H, phen), 8.16 (d, J = 8.4 Hz, 1 H, phen), 7.89 (d, J = 8.7 Hz, 1 H, phen), 7.81 (d, J = 8.7 Hz, 1 H, phen), 7.72–7.62 (m, 3 H, Ph), 7.56–7.49 (m, 3 H, Ph) ppm. ¹³C NMR (100 MHz, CDCl₃): δ = 191.4, 156.5, 153.4, 145.9, 144.6, 138.8, 136.7, 136.6, 132.7, 132.5, 129.8, 129.6, 128.6, 128.3, 127.8, 127.5, 127.3, 125.4, 122.6, 119.6 ppm. C₂₅H₁₆N₂O (360.41): calcd. C 83.31, H 4.47, N 7.77; found C 82.94, H 4.45, N 7.73.

Synthesis of Ligand 1: A mixture of 2-acetyl-9-phenyl-1,10-phenanthroline (225 mg, 0.75 mmol), 2,6-dimethylaniline (184 mg, 1.50 mmol), and *p*-toluenesulfonic acid (80 mg) in toluene (20 mL) was refluxed for 24 h under N₂. The solvent was then evaporated under reduced pressure and the residue was eluted with petroleum ether/ethyl acetate (20:1, v/v) on an alumina column. The second fraction was collected and concentrated to give a yellow solid in 34.6% yield (105 mg). M.p. 190–192 °C. FT-IR (KBr disc): $\tilde{\nu}$ = 3041, 3018, 2914, 1635, 1605, 1590, 1546, 1506, 1485, 1467, 1362, 1293, 1204, 1118, 1091, 855, 761, 739, 687 cm⁻¹. ¹H NMR (300 MHz, CDCl₃): δ = 8.80 (d, J = 8.4 Hz, 1 H, phen), 8.45 (d, J = 7.5 Hz, 2 H, Ph), 8.34 (d, J = 8.7 Hz, 2 H, phen), 8.18 (d, J = 8.4 Hz, 1 H, phen), 7.85 (d, J = 3.9 Hz, 2 H, phen), 7.56 (t, J = 7.5 Hz, 2 H, Ph), 7.47 (t, J = 7.5 Hz, 1 H, Ph), 7.11 (d, J = 7.5 Hz, 2 H, Ar), 6.97 (t, J = 7.5 Hz, 1 H, Ar), 2.62 (s, 3 H, COCH₃), 2.09 (s, 6 H, 2 Me) ppm. ¹³C NMR (75 MHz, CDCl₃): δ = 168.0, 156.9, 155.8, 149.0, 146.0, 145.1, 139.2, 137.1, 136.5, 129.8, 129.6, 128.9, 127.9, 127.8, 127.5, 127.3, 126.1, 125.3, 123.1, 120.6, 119.9, 18.0, 16.7 ppm. C₂₈H₂₃N₃ (401.50): calcd. C 83.76, H 5.77, N 10.47; found C 83.69, H 5.76, N 10.40.

Synthesis of Ligand 2: Ligand 2 was prepared from 2-acetyl-9-phenyl-1,10-phenanthroline (446 mg, 1.50 mmol) and 2,6-diethylaniline (491 mg, 3.20 mmol) as a yellow solid in 44.2% yield (284 mg) in a similar manner to that described for ligand 1. M.p. 181–183 °C. FT-IR (KBr disc): $\tilde{\nu}$ = 3060, 3037, 2960, 2929, 2868, 1639, 1608, 1589, 1546, 1507, 1486, 1452, 1418, 1369, 1296, 1258, 1194, 1119, 1099, 862, 828, 762, 740, 686 cm⁻¹. ¹H NMR (300 MHz, CDCl₃): δ = 8.80 (d, J = 8.4 Hz, 1 H, phen), 8.45 (d, J = 7.5 Hz, 2 H, Ph), 8.33 (d, J = 8.4 Hz, 2 H, phen), 8.17 (d, J = 8.4 Hz, 1 H, phen), 7.80 (d, J = 3.9 Hz, 2 H, phen), 7.56 (t, J = 7.5 Hz, 2 H, Ph), 7.47 (t, J = 7.5 Hz, 1 H, Ph), 7.16 (d, J = 7.2 Hz, 2 H, Ar), 7.07 (t, J = 7.2 Hz, 1 H, Ar), 2.64 (s, 3 H, COCH₃), 2.42 (q, J = 7.2 Hz, 4 H, 2 Et), 1.16 (t, J = 7.2 Hz, 6 H, 2 Et) ppm. ¹³C NMR (75 MHz, CDCl₃): δ = 167.7, 156.9, 155.9, 148.0, 146.0, 145.1, 139.2, 137.1, 136.5, 131.1, 129.8, 129.6, 128.9, 127.8, 127.5, 127.3, 126.1, 126.0, 123.4, 120.5, 119.8, 24.7, 17.0, 13.8 ppm. C₃₀H₂₇N₃ (429.56): calcd. C 83.88, H 6.34, N 9.78; found C 83.66, H 6.40, N 9.60.

Synthesis of Ligand 3: Ligand 3 was prepared from 2-acetyl-9-phenyl-1,10-phenanthroline (298 mg, 1.00 mmol) and 2,6-diisopropylaniline (448 mg, 2.50 mmol) as a yellow solid in 53.1% yield (243 mg) in a similar manner to that described for ligand 1. M.p. 256–258 °C. FT-IR (KBr disc): $\tilde{\nu}$ = 3061, 2962, 2924, 2865, 1635, 1607, 1589, 1579, 1546, 1507, 1486, 1462, 1436, 1420, 1381, 1366, 1294, 1247, 1189, 1117, 1097, 860, 780, 761, 741, 685 cm⁻¹. ¹H NMR (400 MHz, CDCl₃): δ = 8.82 (d, J = 8.4 Hz, 1 H, phen), 8.45 (d, J = 7.6 Hz, 2 H, Ph), 8.33 (dd, J_1 = 8.4 Hz, J_2 = 4.7 Hz, 2 H, phen), 8.17 (d, J = 8.4 Hz, 1 H, phen), 7.88 (d, J = 4.0 Hz, 2 H, phen), 7.56 (t, J = 7.6 Hz, 2 H, Ph), 7.47 (t, J = 7.6 Hz, 1 H, Ph), 7.21 (d, J = 7.6 Hz, 2 H, Ar), 7.13 (t, J = 7.6 Hz, 1 H, Ar), 2.86

(sept, J = 6.8 Hz, 2 H, 2 *i*Pr), 2.66 (s, 3 H, COCH₃), 1.19 (d, J = 6.6 Hz, 6 H, *i*Pr), 1.17 (d, J = 6.5 Hz, 6 H, *i*Pr) ppm. ¹³C NMR (75 MHz, CDCl₃): δ = 167.7, 156.9, 155.8, 146.7, 146.0, 145.2, 139.2, 137.1, 136.5, 135.8, 129.9, 129.7, 129.0, 127.8, 127.5, 127.3, 126.1, 123.7, 123.1, 120.6, 119.9, 28.3, 23.3, 23.0, 17.3 ppm. C₃₂H₃₁N₃ (457.61): calcd. C 83.99, H 6.83, N 9.18; found C 84.00, H 6.84, N 8.98.

Synthesis of Ligand 4: 2-Benzoyl-9-phenyl-1,10-phenanthroline (760 mg, 2.10 mmol), 2,6-dimethylaniline (585 mg, 4.80 mmol), and *p*-toluenesulfonic acid (100 mg) were combined with tetraethyl silicate (5 mL) in a flask. The flask was equipped with a condenser and a Dean–Stark trap and the mixture was heated at about 130 °C for 36 h under N₂. Tetraethyl silicate was then removed under reduced pressure and the residue was eluted with petroleum ether/ethyl acetate (6:1, v/v) on an alumina column. The second fraction was collected and concentrated to give a yellow solid in 38.4% yield (376 mg). M.p. 142–144 °C. FT-IR (KBr disc): $\tilde{\nu}$ = 3055, 2943, 1616, 1589, 1577, 1544, 1505, 1484, 1441, 1368, 1319, 1290, 1207, 1088, 1024, 969, 858, 773, 765, 740, 716, 694 cm⁻¹. ¹H NMR (400 MHz, CDCl₃): δ = 8.87 (d, J = 8.4 Hz, 1 H, phen), 8.37 (d, J = 8.4 Hz, 1 H, phen), 8.26–8.24 (m, 3 H), 8.11 (d, J = 8.4 Hz, 1 H, phen), 7.82 (s, 2 H, phen), 7.57 (d, J = 8.0 Hz, 2 H, Ph), 7.46 (m, 4 H, Ph), 7.38 (t, J = 7.2 Hz, 2 H, Ph), 6.96 (d, J = 7.2 Hz, 2 H, Ar), 6.86 (t, J = 7.2 Hz, 1 H, Ar), 2.12 (s, 6 H, 2 Me) ppm. ¹³C NMR (100 MHz, CDCl₃): δ = 166.1, 155.9, 155.7, 148.2, 145.7, 144.7, 138.5, 136.3, 136.0, 135.4, 129.6, 129.2, 129.1, 128.9, 128.3, 127.9, 127.3, 127.0, 126.8, 126.7, 125.5, 125.2, 122.7, 121.7, 118.9, 18.2 ppm. C₃₃H₂₅N₃ (463.57): calcd. C 85.50, H 5.44, N 9.06; found C 85.14, H 5.47, N 8.94.

Synthesis of Ligand 5: Ligand 5 was prepared from 2-benzoyl-9-phenyl-1,10-phenanthroline (570 mg, 1.58 mmol) and 2,6-diethylaniline (498 mg, 3.27 mmol) as a yellow solid in 72.8% yield (556 mg) in a similar manner to that described for ligand 4. M.p. 187–189 °C. FT-IR (KBr disc): $\tilde{\nu}$ = 3060, 3034, 2962, 2918, 1618, 1586, 1542, 1504, 1485, 1440, 1363, 1294, 1200, 1090, 965, 869, 763, 697 cm⁻¹. ¹H NMR (400 MHz, CDCl₃): δ = 8.85 (d, J = 8.0 Hz, 1 H, phen), 8.37–8.22 (m, 4 H), 8.09 (d, J = 8.0 Hz, 1 H, phen), 7.80 (s, 2 H, phen), 7.58 (s, 2 H, Ph), 7.45–7.36 (m, 6 H, Ph), 7.01–6.97 (m, 3 H, Ar), 2.61 (q, J = 7.2 Hz, 2 H, Et), 2.34 (q, J = 7.2 Hz, 2 H, Et), 1.16 (t, J = 7.2 Hz, 6 H, 2 Et) ppm. ¹³C NMR (100 MHz, CDCl₃): δ = 165.7, 156.2, 156.1, 147.6, 146.1, 145.1, 138.9, 136.7, 136.4, 135.4, 131.1, 130.3, 129.6, 129.2, 128.7, 128.5, 127.7, 127.5, 127.3, 127.2, 125.8, 125.5, 123.4, 122.1, 119.2, 24.5, 13.5 ppm. C₃₅H₂₉N₃ (491.62): calcd. C 85.51, H 5.95, N 8.55; found C 85.03, H 5.94, N 8.48.

Synthesis of Ligand 6: Ligand 6 was prepared from 2-benzoyl-9-phenyl-1,10-phenanthroline (394 mg, 1.09 mmol) and 2,6-diisopropylaniline (433 mg, 2.44 mmol) as a yellow solid in 74.0% yield (420 mg) in a similar manner to that described for ligand 4. M.p. 170–171 °C. FT-IR (KBr disc): $\tilde{\nu}$ = 3063, 2958, 2860, 1611, 1588, 1544, 1506, 1487, 1463, 1430, 1358, 1291, 1194, 1091, 966, 858, 777, 757, 701 cm⁻¹. ¹H NMR (300 MHz, CDCl₃): δ = 8.84 (d, J = 8.4 Hz, 1 H, phen), 8.38–8.24 (m, 4 H), 8.11 (d, J = 8.4 Hz, 1 H, phen), 7.82 (s, 2 H, phen), 7.62 (m, 2 H, Ph), 7.49–7.39 (m, 6 H, Ph), 7.04 (m, 3 H, Ar), 3.00 (sept, J = 6.8 Hz, 2 H, 2 *i*Pr), 1.19 (d, J = 6.8 Hz, 6 H, *i*Pr), 0.97 (d, J = 6.8 Hz, 6 H, *i*Pr) ppm. ¹³C NMR (100 MHz, CDCl₃): δ = 164.9, 155.9, 145.7, 144.6, 138.5, 136.3, 136.0, 135.2, 134.5, 130.3, 129.1, 128.7, 128.4, 128.2, 128.1, 127.2, 127.1, 126.9, 126.7, 125.4, 123.2, 122.4, 121.8, 111.8, 28.1, 23.7, 21.6 ppm. C₃₇H₃₃N₃ (519.68): calcd. C 85.51, H 6.40, N 8.09; found C 84.91, H 6.36, N 7.84.

Synthesis of Iron Complexes 1a–6a. General Procedure: The ligand (0.20 mmol) and one equiv. of FeCl₂·4H₂O (0.20 mmol) were

placed in a Schlenk tube, which was purged three times with nitrogen and then charged with thf. The reaction mixture was then stirred at room temperature for 9 h. The resulting precipitate was filtered, washed with diethyl ether, and dried in vacuo. All the iron(II) complexes were isolated in high yield.

Complex 1a: Isolated as a green powder in 98.4% yield (104 mg). FT-IR (KBr disc): $\tilde{\nu}$ = 3059, 2953, 2918, 2867, 1615, 1590, 1555, 1504, 1491, 1468, 1451, 1435, 1374, 1299, 1205, 865, 792, 772, 745, 702 cm^{-1} . $\text{C}_{28}\text{H}_{23}\text{Cl}_2\text{FeN}_3 \cdot 1/2\text{CH}_2\text{Cl}_2$ (570.72): calcd. C 59.98, H 4.24, N 7.36; found C 59.61, H 4.34, N 7.28.

Complex 2a: Isolated as a green powder in 95.9% yield (107 mg). FT-IR (KBr disc): $\tilde{\nu}$ = 3063, 2966, 2929, 2872, 1617, 1584, 1558, 1504, 1490, 1442, 1374, 1289, 1243, 1205, 1193, 1152, 1141, 1060, 859, 786, 759, 744, 701 cm^{-1} . $\text{C}_{30}\text{H}_{27}\text{Cl}_2\text{FeN}_3$ (556.31): calcd. C 64.77, H 4.89, N 7.55; found C 64.26, H 4.59, N 7.50.

Complex 3a: Isolated as a green powder in 66.2% yield (78 mg). FT-IR (KBr disc): $\tilde{\nu}$ = 3062, 2969, 2926, 2865, 1611, 1590, 1557, 1501, 1490, 1463, 1440, 1374, 1330, 1286, 1247, 1185, 1152, 1138, 870, 786, 748, 701 cm^{-1} . $\text{C}_{32}\text{H}_{31}\text{Cl}_2\text{FeN}_3$ (584.36): calcd. C 65.77, H 5.35, N 7.19; found C 65.15, H 5.32, N 6.95.

Complex 4a: Isolated as a gray-green powder in 86.9% yield (103 mg). FT-IR (KBr disc): $\tilde{\nu}$ = 3056, 2922, 1620, 1588, 1549, 1489, 1445, 1368, 1300, 1212, 1155, 1001, 863, 774, 744, 703 cm^{-1} . $\text{C}_{33}\text{H}_{25}\text{Cl}_2\text{FeN}_3 \cdot \text{H}_2\text{O}$ (608.34): calcd. C 65.15, H 4.47, N 6.91; found C 65.12, H 4.11, N 6.85.

Complex 5a: Isolated as a brown powder in 79.8% yield (99 mg). FT-IR (KBr disc): $\tilde{\nu}$ = 3061, 2966, 2874, 1594, 1553, 1490, 1444, 1368, 1291, 1261, 1107, 1059, 1000, 868, 781, 702 cm^{-1} . $\text{C}_{35}\text{H}_{29}\text{Cl}_2\text{FeN}_3$ (618.38): calcd. C 67.98, H 4.73, N 6.80; found C 67.94, H 4.78, N 6.57.

Complex 6a: Isolated as a green powder in 86.6% yield (112 mg). FT-IR (KBr disc): $\tilde{\nu}$ = 3031, 2959, 2866, 1620, 1587, 1550, 1488, 1459, 1436, 1364, 1319, 1274, 1206, 995, 872, 850, 704 cm^{-1} . $\text{C}_{37}\text{H}_{33}\text{Cl}_2\text{FeN}_3$ (646.43): calcd. C 68.75, H 5.15, N 6.50; found C 68.42, H 5.23, N 6.59.

Synthesis of Cobalt Complexes 1b–6b and Nickel Complexes 1c–6c.

General Procedure: The ligand (0.20 mmol) and one equiv. of CoCl_2 or $\text{NiCl}_2 \cdot 6\text{H}_2\text{O}$ (0.20 mmol) were placed in a Schlenk tube along with anhydrous ethanol. The reaction mixture was then stirred at room temperature for 9 h. The resulting precipitate was filtered, washed with diethyl ether, and dried in vacuo. All the complexes were isolated in high yield.

Complex 1b: Isolated as a green powder in 65.6% yield (70 mg). FT-IR (KBr disc): $\tilde{\nu}$ = 3063, 2945, 2914, 1619, 1585, 1557, 1504, 1490, 1451, 1437, 1374, 1290, 1256, 1206, 1142, 989, 919, 865, 791, 772, 745, 700, 653, 609 cm^{-1} . $\text{C}_{28}\text{H}_{23}\text{Cl}_2\text{CoN}_3 \cdot \text{H}_2\text{O}$ (549.36): calcd. C 61.22, H 4.59, N 7.65; found C 61.46, H 4.34, N 7.24.

Complex 2b: Isolated as a green powder in 80.3% yield (91 mg). FT-IR (KBr disc): $\tilde{\nu}$ = 3061, 2969, 2924, 2865, 1613, 1582, 1557, 1501, 1489, 1463, 1441, 1375, 1330, 1288, 1185, 1153, 869, 786, 749, 700 cm^{-1} . $\text{C}_{30}\text{H}_{27}\text{Cl}_2\text{CoN}_3$ (559.39): calcd. C 64.41, H 4.86, N 7.51; found C 64.25, H 4.92, N 7.27.

Complex 3b: Isolated as a green powder in 85.6% yield (103 mg). FT-IR (KBr disc): $\tilde{\nu}$ = 3450, 3062, 2964, 2932, 2875, 1618, 1585, 1558, 1504, 1490, 1441, 1375, 1290, 1193, 859, 787, 760, 745, 701 cm^{-1} . $\text{C}_{32}\text{H}_{31}\text{Cl}_2\text{CoN}_3$ (587.45): calcd. C 65.43, H 5.32, N 7.15; found C 64.48, H 5.55, N 6.61.

Complex 4b: Isolated as a red-brown powder in 80.2% yield (95 mg). FT-IR (KBr disc): $\tilde{\nu}$ = 3057, 2919, 1612, 1597, 1555, 1490,

1445, 1371, 1317, 1289, 1213, 999, 863, 774, 748, 721, 703 cm^{-1} . $\text{C}_{33}\text{H}_{25}\text{Cl}_2\text{CoN}_3 \cdot \text{CH}_2\text{Cl}_2$ (678.34): calcd. C 60.20, H 4.01, N 6.19; found C 60.25, H 4.02, N 6.28.

Complex 5b: Isolated as a red-brown powder in 77.6% yield (84 mg). FT-IR (KBr disc): $\tilde{\nu}$ = 3063, 2963, 2934, 2875, 1613, 1596, 1552, 1498, 1490, 1442, 1371, 1319, 1288, 1108, 995, 872, 782, 751, 720, 701 cm^{-1} . $\text{C}_{35}\text{H}_{29}\text{Cl}_2\text{CoN}_3 \cdot \text{CH}_2\text{Cl}_2$ (706.40): calcd. C 61.21, H 4.42, N 5.95; found C 60.68, H 4.28, N 5.63.

Complex 6b: Isolated as a red-brown powder in 78.4% yield (103 mg). FT-IR (KBr disc): $\tilde{\nu}$ = 3058, 3032, 2959, 2924, 2865, 1619, 1599, 1552, 1489, 1437, 1370, 1319, 1274, 1207, 1100, 995, 873, 850, 759, 718, 652 cm^{-1} . $\text{C}_{37}\text{H}_{33}\text{Cl}_2\text{CoN}_3 \cdot \text{CH}_2\text{Cl}_2$ (734.45): calcd. C 62.14, H 4.80, N 5.72; found C 62.17, H 4.82, N 5.54.

Complex 1c: Isolated as an orange powder in 89.3% yield (95 mg). FT-IR (KBr disc): $\tilde{\nu}$ = 3445, 3056, 1611, 1587, 1556, 1503, 1489, 1453, 1376, 1294, 1204, 1148, 862, 793, 773, 745, 702 cm^{-1} . $\text{C}_{28}\text{H}_{23}\text{Cl}_2\text{Ni} \cdot 1/2\text{CH}_2\text{Cl}_2$ (573.57): calcd. C 59.68, H 4.22, N 7.33; found C 59.89, H 4.44, N 7.20.

Complex 2c: Isolated as an orange powder in 89.7% yield (100 mg). FT-IR (KBr disc): $\tilde{\nu}$ = 3442, 3062, 2958, 2871, 1616, 1584, 1559, 1502, 1489, 1442, 1377, 1302, 1292, 1192, 1060, 859, 787, 762, 744, 701 cm^{-1} . $\text{C}_{30}\text{H}_{27}\text{Cl}_2\text{Ni} \cdot 1/2\text{CH}_2\text{Cl}_2$ (601.62): calcd. C 60.89, H 4.69, N 6.98; found C 60.46, H 4.96, N 6.67.

Complex 3c: Isolated as an orange powder in 76.5% yield (90 mg). FT-IR (KBr disc): $\tilde{\nu}$ = 3426, 3060, 2967, 2865, 1609, 1586, 1558, 1489, 1443, 1378, 1330, 1293, 1185, 1151, 869, 787, 761, 749, 702 cm^{-1} . $\text{C}_{32}\text{H}_{31}\text{Cl}_2\text{Ni} \cdot \text{CH}_2\text{Cl}_2$ (672.14): calcd. C 58.97, H 4.95, N 6.25; found C 58.44, H 5.02, N 6.20.

Complex 4c: Isolated as a yellow powder in 96.0% yield (114 mg). FT-IR (KBr disc): $\tilde{\nu}$ = 3388, 1618, 1592, 1554, 1486, 1445, 1378, 1290, 1212, 1057, 1038, 1004, 868, 778, 754, 723, 703 cm^{-1} . $\text{C}_{33}\text{H}_{25}\text{Cl}_2\text{Ni} \cdot \text{H}_2\text{O}$ (611.19): calcd. C 64.85, H 4.45, N 6.88; found C 65.09, H 4.16, N 6.82.

Complex 5c: Isolated as an orange powder in 90.6% yield (113 mg). FT-IR (KBr disc): $\tilde{\nu}$ = 3061, 2963, 1597, 1558, 1489, 1443, 1377, 1291, 1209, 1148, 1108, 1065, 1040, 1004, 867, 784, 706 cm^{-1} . $\text{C}_{35}\text{H}_{29}\text{Cl}_2\text{Ni} \cdot 1/2\text{CH}_2\text{Cl}_2$ (663.69): calcd. C 64.24, H 4.56, N 6.33; found C 64.50, H 4.75, N 6.60.

Complex 6c: Isolated as an orange powder in 75.1% yield (98 mg). FT-IR (KBr disc): $\tilde{\nu}$ = 3440, 3057, 2962, 2866, 1621, 1595, 1554, 1490, 1439, 1377, 1322, 1293, 1207, 1151, 1101, 1024, 872, 784, 763, 707 cm^{-1} . $\text{C}_{37}\text{H}_{33}\text{Cl}_2\text{Ni} \cdot 1/2\text{CH}_2\text{Cl}_2$ (691.75): calcd. C 65.11, H 4.95, N 6.07; found C 65.01, H 5.04, N 5.85.

General Procedure for Ethylene Oligomerization at 1 atm of Ethylene Pressure:

A flame-dried, three-necked flask was loaded with the catalyst precursor and purged three times with nitrogen. Ethylene was then charged in the flask along with freshly distilled toluene and the mixture stirred for 10 min under 1 atm of ethylene pressure. The reaction temperature was controlled with a water bath and the required amount of co-catalyst was then injected with a syringe. The reaction mixture was stirred for the required time and then the reaction was quenched by addition of 5% aqueous hydrogen chloride. The contents and distributions of oligomers were determined by GC.

General Procedure for Ethylene Oligomerization at 10 Atm of Ethylene Pressure:

A 250-mL stainless steel reactor equipped with a mechanical stirrer and a temperature controller was heated in vacuo for at least 2 h at above 80 °C, then cooled to the required reaction temperature under ethylene atmosphere and charged with toluene, the desired amount of co-catalyst, and a toluene solution of the

Table 6. Crystal data and structure refinement for **1b**, **2**, **2a**, and **4b**.

	1b	2	2a	4b
CCDC number	650187	650185	650186	650188
Formula	C ₂₈ H ₂₃ Cl ₂ CoN ₃ O	C ₃₀ H ₂₇ N ₃	C ₃₀ H ₂₇ Cl ₂ FeN ₃ O _{0.5}	C ₃₃ H ₂₅ Cl ₂ CoN ₃ ·CH ₂ Cl ₂
Formula weight	547.32	429.55	564.30	678.32
Temperature [K]	293(2)	294(2)	293(2)	294(2)
Wavelength [Å]	0.71073	0.71073	0.71073	0.71073
Crystal system	monoclinic	triclinic	triclinic	triclinic
Space group	C2/c	P $\bar{1}$	P $\bar{1}$	P $\bar{1}$
<i>a</i> [Å]	25.9027(8)	7.869(2)	13.3880(6)	8.6610(14)
<i>b</i> [Å]	16.9116(6)	11.840(3)	14.0560(6)	9.5741(15)
<i>c</i> [Å]	16.5805(5)	13.547(4)	14.9754(6)	19.014(3)
α [°]	90	105.675(5)	83.065(3)	81.376(2)
β [°]	128.031(2)	94.203(5)	86.114(3)	88.499(3)
γ [°]	90	99.069(5)	78.191(3)	86.065(3)
<i>V</i> [Å ³]	5721.0(3)	1191.1(6)	2735.6(2)	1555.0(4)
<i>Z</i>	8	2	4	2
<i>D</i> _{calcd.} [g cm ⁻³]	1.271	1.198	1.370	1.449
μ [mm ⁻¹]	0.810	0.071	0.772	0.925
<i>F</i> (000)	2248	456	1168	694
Crystal size [mm]	0.26 × 0.20 × 0.15	0.24 × 0.15 × 0.12	0.20 × 0.14 × 0.12	0.25 × 0.12 × 0.08
θ range [°]	2.46–28.32	1.82–26.49	1.37–28.36	1.08–26.45
Limiting indices	–34 ≤ <i>h</i> ≤ 34 –22 ≤ <i>k</i> ≤ 22 –21 ≤ <i>l</i> ≤ 22	–9 ≤ <i>h</i> ≤ 5 –14 ≤ <i>k</i> ≤ 14 –16 ≤ <i>l</i> ≤ 15	–17 ≤ <i>h</i> ≤ 17 –18 ≤ <i>k</i> ≤ 18 –19 ≤ <i>l</i> ≤ 19	–10 ≤ <i>h</i> ≤ 7 –10 ≤ <i>k</i> ≤ 11 –23 ≤ <i>l</i> ≤ 19
% Completeness to θ	99.1 (θ = 28.32°)	97.7 (θ = 26.49°)	98.8 (θ = 28.36°)	97.7 (θ = 26.45°)
Absorption correction	empirical	empirical	empirical	empirical
No. of parameters	334	302	667	379
Goodness-of-fit on <i>F</i> ²	0.931	0.981	0.734	1.018
<i>R</i> 1 [<i>I</i> > 2σ(<i>I</i>)]	0.0672	0.0538	0.0494	0.0522
<i>wR</i> 2	0.1895	0.1183	0.1191	0.1208
Largest diff. peak/hole [e Å ⁻³]	0.915/–0.349	0.121/–0.171	0.381/–0.374	0.491/–0.499

Table 7. Crystal data and structure refinement for **1c**, **5c**, and **6b**.

	1c	5c	6b
CCDC number	650190	650191	650189
Formula	C ₂₈ H ₂₃ Cl ₂ N ₃ Ni·CH ₂ Cl ₂	C ₃₅ H ₂₉ Cl ₂ N ₃ Ni·2CH ₂ Cl ₂	C ₃₇ H ₃₃ Cl ₂ CoN ₃ ·CH ₂ Cl ₂
Formula weight	616.03	791.07	734.42
Temperature [K]	293(2)	293(2)	293(2)
Wavelength [Å]	0.71073	0.71073	0.71073
Crystal system	monoclinic	triclinic	triclinic
Space group	P2 ₁ /c	P $\bar{1}$	P $\bar{1}$
<i>a</i> [Å]	18.870(4)	9.2599(4)	9.2300(18)
<i>b</i> [Å]	9.7077(19)	9.6246(4)	10.254(2)
<i>c</i> [Å]	15.550(3)	20.9828(9)	17.912(4)
α [°]	90	97.054(2)	96.51(3)
β [°]	96.26(3)	95.194(2)	90.33(3)
γ [°]	90	98.629(2)	92.04(3)
<i>V</i> [Å ³]	2831.6(10)	1823.54(13)	1683.2(6)
<i>Z</i>	4	2	2
<i>D</i> _{calcd.} [g cm ⁻³]	1.445	1.441	1.449
μ [mm ⁻¹]	1.086	1.003	0.860
<i>F</i> (000)	1264	812	758
Crystal size [mm]	0.26 × 0.19 × 0.11	0.31 × 0.22 × 0.20	0.30 × 0.18 × 0.12
θ range [°]	2.17–25.01	0.98–28.35	1.14–26.47
Limiting indices	–19 ≤ <i>h</i> ≤ 22 –11 ≤ <i>k</i> ≤ 1 –18 ≤ <i>l</i> ≤ 18	–12 ≤ <i>h</i> ≤ 12 –10 ≤ <i>k</i> ≤ 12 –27 ≤ <i>l</i> ≤ 27	–11 ≤ <i>h</i> ≤ 11 –12 ≤ <i>k</i> ≤ 10 –17 ≤ <i>l</i> ≤ 22
% Completeness to θ	100.0 (θ = 25.01°)	98.7 (θ = 28.35°)	97.4 (θ = 26.47°)
Absorption correction	empirical	empirical	empirical
No. of parameters	334	424	415
Goodness-of-fit on <i>F</i> ²	1.00	0.87	1.038
<i>R</i> 1 [<i>I</i> > 2σ(<i>I</i>)]	0.0917	0.0614	0.0452
<i>wR</i> 2	0.1527	0.1661	0.1048
Largest diff. peak/hole [e Å ⁻³]	0.360/–0.407	0.540/–0.531	0.697/–0.629

catalyst precursor; the total volume was 100 mL. The reactor was sealed and pressurized to 10 atm of ethylene pressure at the required reaction temperature, and the ethylene pressure was maintained with a feed of ethylene. After the required time the pressure was released. A small amount of the reaction solution was collected and the reaction quenched by addition of 5% aqueous hydrogen chloride. The organic layer was analyzed by GC to determine the composition and mass distribution of the oligomers obtained. Finally, the remaining reaction solution was quenched with 5% hydrochloric acid in ethanol.

X-ray Crystallography: Single-crystal X-ray diffraction studies for **1b**, **1c**, **2a**, and **5c** were carried out with a Bruker P4 diffractometer with graphite-monochromated Mo- K_α radiation ($\lambda = 0.71073 \text{ \AA}$) at 293(2) K. Intensity data for crystals of **2**, **4b** and **6b** were collected with a Bruker SMART 1000 CCD diffractometer with graphite-monochromated Mo- K_α radiation ($\lambda = 0.71073 \text{ \AA}$). Cell parameters were obtained by global refinement of the positions of all collected reflections. Intensities were corrected for Lorentz and polarization effects and empirical absorption. The structures were solved by direct methods and refined by full-matrix least-squares on F^2 . All non-hydrogen atoms were refined anisotropically. All hydrogen atoms were placed in calculated positions. Structure solution and refinement were performed with the SHELXL-97 package.^[28] Crystallographic data and processing parameters for **1b**, **1c**, **2**, **2a**, **4b**, **5c**, and **6b** are summarized in Tables 6 and 7.

CCDC-650185 to -650191 contain the supplementary crystallographic data for this paper, which could be obtained free of charge from the Cambridge Crystallographic Data Centre via www.ccdc.cam.ac.uk/data_request/cif.

Acknowledgments

This project was supported by the National Natural Science Foundation of China (grant nos. 20473099 and 20674089). We thank Mr. Saliu Alao Amolegbe (a CAS-TWAS Postgraduate Fellow from Nigeria) for English corrections.

- [1] a) D. Vogt, *Applied Homogeneous Catalysis with Organometallic Compounds* (Eds.: B. Cornils, W. A. Herrmann), VCH, Weinheim, **2002**, vol. 1, p. 240–253; b) A. M. Al-Jarallah, J. A. Anabtawi, M. A. B. Siddiqui, A. M. Aitani, A. W. Al-Sa'doun, *Catal. Today* **1992**, *14*, 1–121.
- [2] a) W. Keim, F. H. Kowaldt, R. Goddard, C. Krüger, *Angew. Chem. Int. Ed. Engl.* **1978**, *17*, 466–467; b) W. Keim, *Angew. Chem. Int. Ed. Engl.* **1990**, *29*, 235–244; c) P. Braunstein, Y. Chauvin, S. Mercier, L. Saussine, A. D. Cian, J. Fisher, *J. Chem. Soc. Chem. Commun.* **1994**, 2203–2204; d) J. Heinicke, M. He, A. Dal, H.-F. Klein, O. Hetche, W. Keim, U. Flörke, H.-J. Haupt, *Eur. J. Inorg. Chem.* **2000**, 431–440.
- [3] a) G. J. P. Britovsek, V. C. Gibson, D. F. Wass, *Angew. Chem. Int. Ed.* **1999**, *38*, 428–447; b) S. D. Ittel, L. K. Johnson, M. Brookhart, *Chem. Rev.* **2000**, *100*, 1169–1203; c) V. C. Gibson, S. K. Spitzmesser, *Chem. Rev.* **2003**, *103*, 283–316; d) W. Zhang, W. Zhang, W.-H. Sun, *Prog. Chem.* **2005**, *17*, 310–319; e) S. Jie, S. Zhang, W.-H. Sun, *Petrochem. Tech. (Shiyou Huagong)* **2006**, *35*, 295–300.
- [4] a) C. Bianchini, G. Giambastiani, I. G. Rios, G. Mantovani, A. Meli, A. M. Segarra, *Coord. Chem. Rev.* **2006**, *250*, 1391–1418 and references therein; b) V. C. Gibson, C. Redshaw, G. A. Solan, *Chem. Rev.* **2007**, *107*, 1745–1776 and references therein.
- [5] a) F. Speiser, P. Braunstein, L. Saussine, *Acc. Chem. Res.* **2005**, *38*, 784–793; b) W.-H. Sun, D. Zhang, S. Zhang, S. Jie, J. Hou, *Kinet. Catal.* **2006**, *47*, 278–283.
- [6] a) L. K. Johnson, C. M. Killian, M. Brookhart, *J. Am. Chem. Soc.* **1995**, *117*, 6414–6415; b) D. P. Gates, S. A. Svejda, E. Oñate, C. M. Killian, L. K. Johnson, P. S. White, M. Brookhart, *Macromolecules* **2000**, *33*, 2320–2334.
- [7] a) X. Tang, W.-H. Sun, T. Gao, J. Hou, J. Chen, W. Chen, *J. Organomet. Chem.* **2005**, *690*, 1570–1580; b) Q.-Z. Yang, A. Kermagoret, M. Agostinho, O. Siri, P. Braunstein, *Organometallics* **2006**, *25*, 5518–5527.
- [8] F. Speiser, P. Braunstein, L. Saussine, *Dalton Trans.* **2004**, 1539–1545.
- [9] a) J. Hou, W.-H. Sun, S. Zhang, H. Ma, Y. Deng, X. Lu, *Organometallics* **2006**, *25*, 236–244; b) C. Zhang, W.-H. Sun, Z.-X. Wang, *Eur. J. Inorg. Chem.* **2006**, *23*, 4895–4902.
- [10] a) D. M. Dawson, D. A. Walker, M. Thornton-Pett, M. Bochmann, *J. Chem. Soc. Dalton Trans.* **2000**, 459–466; b) S. Al-Benna, M. J. Sarsfield, M. Thornton-Pett, D. Ormsby, P. J. Maddox, P. Bres, M. Bochmann, *J. Chem. Soc. Dalton Trans.* **2000**, 4247–4257; c) F. A. Kunrath, R. F. de Souza, O. L. Casagrande Jr, N. R. Brooks, V. G. Young Jr, *Organometallics* **2003**, *22*, 4739–4743; d) N. Ajellal, M. C. A. Kuhn, A. D. G. Boff, M. Hörner, C. M. Thomas, J.-F. Carpentier, O. L. Casagrande Jr, *Organometallics* **2006**, *25*, 1213–1216.
- [11] L. Wang, W.-H. Sun, L. Han, H. Yang, Y. Hu, X. Jin, *J. Organomet. Chem.* **2002**, *658*, 62–70.
- [12] W.-H. Sun, S. Zhang, S. Jie, W. Zhang, Y. Li, H. Ma, J. Chen, K. Wedeking, R. Fröhlich, *J. Organomet. Chem.* **2006**, *691*, 4196–4203.
- [13] M. Zhang, S. Zhang, P. Hao, S. Jie, W.-H. Sun, P. Li, X. Lu, *Eur. J. Inorg. Chem.* **2007**, 3816.
- [14] a) P. Hao, S. Zhang, W.-H. Sun, Q. Shi, S. Adewuyi, X. Lu, P. Li, *Organometallics* **2007**, *26*, 2439–2446; b) S. Adewuyi, G. Li, S. Zhang, W. Wang, P. Hao, W.-H. Sun, N. Tang, J. Yi, *J. Organomet. Chem.* **2007**, *692*, 3532–3541.
- [15] a) S. Zhang, I. Vystorop, Z. Tang, W.-H. Sun, *Organometallics* **2007**, *26*, 2456–2460; b) S. Zhang, W.-H. Sun, X. Kuang, I. Vystorop, J. Yi, *J. Organomet. Chem.* **2007**, *692*, 5307–5316; c) W.-H. Sun, P. Hao, S. Zhang, Q. Shi, W. Zuo, X. Tang, *Organometallics* **2007**, *26*, 2720–2734; d) W.-H. Sun, P. Hao, G. Li, S. Zhang, W. Wang, J. Yi, M. Asma, N. Tang, *J. Organomet. Chem.* **2007**, *692*, 4506–4518.
- [16] a) B. L. Small, M. Brookhart, A. M. A. Bennett, *J. Am. Chem. Soc.* **1998**, *120*, 4049–4050; b) B. L. Small, M. Brookhart, *J. Am. Chem. Soc.* **1998**, *120*, 7143–7144; c) G. J. P. Britovsek, V. C. Gibson, B. S. Kimberley, P. J. Maddox, S. J. McTavish, G. A. Solan, A. J. P. White, D. J. Williams, *Chem. Commun.* **1998**, 849–850; d) G. J. P. Britovsek, M. Bruce, V. C. Gibson, B. S. Kimberley, P. J. Maddox, S. Mastroianni, S. J. McTavish, C. Redshaw, G. A. Solan, S. Stromberg, A. J. P. White, D. J. Williams, *J. Am. Chem. Soc.* **1999**, *121*, 8728–8740.
- [17] a) G. J. P. Britovsek, V. C. Gibson, O. D. Hoarau, S. K. Spitzmesser, A. J. P. White, D. J. Williams, *Inorg. Chem.* **2003**, *42*, 3454–3465; b) V. C. Gibson, S. K. Spitzmesser, A. J. P. White, D. J. Williams, *Dalton Trans.* **2003**, 2718–2727; c) R. Cowdell, C. J. Davies, S. J. Hilton, J.-D. Maréchal, G. A. Solan, O. Thomas, J. Fawcett, *Dalton Trans.* **2004**, 3231–3240.
- [18] a) G. J. P. Britovsek, S. P. D. Baugh, O. Hoarau, V. C. Gibson, D. F. Wass, A. J. P. White, D. J. Williams, *Inorg. Chim. Acta* **2003**, *345*, 279–291; b) Y. Nakayama, Y. Baba, H. Yasuda, K. Kawakita, N. Ueyama, *Macromolecules* **2003**, *36*, 7953–7958; c) C. J. Davies, S. J. Hilton, G. A. Solan, W. Stannard, J. Fawcett, *Polyhedron* **2005**, *24*, 2017–2026; d) J. D. A. Pelletier, Y. D. M. Champouret, J. Cadarso, L. Clowes, M. Ganete, K. Singh, V. Thanarajasingham, G. A. Solan, *J. Organomet. Chem.* **2006**, *691*, 4114–4123.
- [19] a) W.-H. Sun, S. Jie, S. Zhang, W. Zhang, Y. Song, H. Ma, J. Chen, K. Wedeking, R. Fröhlich, *Organometallics* **2006**, *25*, 666–677; b) S. Jie, S. Zhang, W.-H. Sun, X. Kuang, T. Liu, J. Guo, *16961 J. Mol. Catal. A: Chem.* **2007**, *269*, 85–96; c) S. Zhang, S. Jie, Q. Shi, W.-H. Sun, *J. Mol. Catal. A: Chem.* **2007**, *276*, 174–183.

- [20] S. Jie, S. Zhang, K. Wedeking, W. Zhang, H. Ma, X. Lu, Y. Deng, W.-H. Sun, *C. R. Chim.* **2006**, 9, 1500–1509.
- [21] E. J. Corey, A. L. Borror, T. Foglia, *J. Org. Chem.* **1965**, 30, 288–290.
- [22] A. J. Showler, P. A. Darley, *Chem. Rev.* **1967**, 67, 427–440.
- [23] C. Dietrich-Buchecker, B. Colasson, D. Jouvenot, J.-P. Sauvage, *Chem. Eur. J.* **2005**, 11, 4374–4386.
- [24] K. Ziegler, H. G. Gellert, *Justus Liebigs Ann. Chem.* **1950**, 567, 179–185.
- [25] J. Einhorn, J. L. Luche, *Tetrahedron Lett.* **1986**, 26, 501–504.
- [26] a) C. Carlini, M. Isola, V. Liuzzo, A. M. R. Galletti, G. Sbrana, *Appl. Catal. A* **2002**, 231, 307–320; b) J. C. Jenkins, M. Brookhart, *Organometallics* **2003**, 22, 250–256; c) W.-H. Sun, W. Zhang, T. Gao, X. Tang, L. Chen, Y. Li, X. Jin, *J. Organomet. Chem.* **2004**, 689, 917–929.
- [27] a) C. M. Killian, L. K. Johnson, M. Brookhart, *Organometallics* **1997**, 16, 2005–2007; b) S. A. Svejda, M. Brookhart, *Organometallics* **1999**, 18, 65–74.
- [28] G. M. Sheldrick, *SHELXL-97, Program for the Refinement of Crystal Structures*, University of Göttingen, Germany, **1997**.

Received: July 2, 2007

Published Online: October 24, 2007